Artificial intelligence performance in detecting tumor metastasis from medical radiology imaging: A systematic review and meta-analysis

Qiuhan Zheng[a,b,1], Le Yang[a,b,1], Bin Zeng[a,b], Jiahao Li[a,b], Kaixin Guo[a,b], Yujie Liang[a,b,#,*], Guiqing Liao[a,b,#,*]

[a] Department of Oral and Maxillofacial Surgery, Guanghua School of Stomatology, Hospital of Stomatology, Sun Yat-sen University, Guangzhou, China
[b] Guangdong Provincial Key Laboratory of Stomatology, Guangzhou, China

ARTICLE INFO

ABSTRACT

Background: Early diagnosis of tumor metastasis is crucial for clinical treatment. Artificial intelligence (AI) has shown great promise in the field of medicine. We therefore aimed to evaluate the diagnostic accuracy of AI algorithms in detecting tumor metastasis using medical radiology imaging.

Methods: We searched PubMed and Web of Science for studies published from January 1, 1997, to January 30, 2020. Studies evaluating an AI model for the diagnosis of tumor metastasis from medical images were included. We excluded studies that used histopathology images or medical wave-form data and those focused on the region segmentation of interest. Studies providing enough information to construct contingency tables were included in a meta-analysis.

Findings: We identified 2620 studies, of which 69 were included. Among them, 34 studies were included in a meta-analysis with a pooled sensitivity of 82% (95% CI 79−84%), specificity of 84% (82−87%) and AUC of 0·90 (0·87−0·92). Analysis for different AI algorithms showed a pooled sensitivity of 87% (83−90%) for machine learning and 86% (82−89%) for deep learning, and a pooled specificity of 89% (82−93%) for machine learning, and 87% (82−91%) for deep learning.

Interpretation: AI algorithms may be used for the diagnosis of tumor metastasis using medical radiology imaging with equivalent or even better performance to health-care professionals, in terms of sensitivity and specificity. At the same time, rigorous reporting standards with external validation and comparison to health-care professionals are urgently needed for AI application in the medical field.

Funding: College students' innovative entrepreneurial training plan program .

1. Introduction

Tumor metastasis, including lymph node metastasis (LNM) and distant metastasis (DM), contributes to cancer-related death. Regarding tumor classification, N and M staging are essential for both the treatment strategy, like the plan for surgery and chemoradiotherapy, and prognosis prediction [1,2]. Thus, it is crucial to conduct a complete and accurate pre-operative clinical evaluation of tumor metastasis.

Medical imaging is commonly used to visualize tumor dissemination and quantify the severity, providing valuable information for diagnosis, staging and treatment decision [3] with satisfactory diagnostic accuracy. For example, the sensitivity and specificity of contrast-enhanced ultrasound (CEUS), multidetector computed tomography (MDCT), magnetic resonance imaging (MRI), and fluoro-deoxyglucose (FDG) positron emission tomography (PET)/CT in the detection of colorectal cancer liver metastasis was 80−97% [4], which is similar in other diseases [5,6]. However, owing to the uncoordinated ratio of doctors to patients and the difficulty of radiological diagnosis, making a correct and timely diagnosis from medical imaging is challenging [7].

Artificial intelligence (AI) has already shown great promise to address this problem through automated diagnosis from medical imaging [8,9]. In the 1980s, artificial neural networks (ANNs) were developed [10], resulting in a surge of machine learning (ML) based on statistical models. In the 1990s, various ML models were successively proposed, such as support vector machines (SVM) [11] and random forests (RF) [12]. It is not until 2006 that deep learning (DL), a new branch of ML, gained great attention [13,14]. Since then, DL, such as convolutional neural networks (CNN) and deep neural networks (DNN), has been applied in many fields, including photo

* Corresponding author.
E-mail addresses: yujie0350@126.com (Y. Liang), drliaoguiqing@hotmail.com (G. Liao).
[1] Joint first authors.
[#] Joint corresponding authors.

Research in context

Evidence before this study

The accurate diagnosis of tumor metastasis without misdiagnosis and missed diagnosis is a challenging task. Artificial intelligence (AI) has already shown great promise for automated diagnosis from medical imaging with rapid speed and high accuracy. There is an urgent need for the application of such diagnostic technologies for the detection of tumor metastasis from medical radiology imaging. We searched PubMed and Web of Science for studies published from Jan 1, 1997, to Jan 30, 2020, with no restrictions on regions, languages, or publication types. Studies were included if they evaluated an AI model for the diagnosis of tumor metastasis from medical images. We found one systematic review comparing performance of AI algorithms with health-care professionals for all diseases, but we did not find systematic reviews focusing on tumor metastasis.

Added value of this study

To the best of our knowledge, this systematic review and meta-analysis is the first to show that AI algorithms were beneficial for the diagnosis of tumor metastasis from medical radiology imaging across a broad range of primary tumors and metastasis sites. During the process, we also found several common methodological defects that should be considered by algorithm developers. High-quality evidence with externally validated results and comparison to health-care professionals are urgently needed for studies on AI application in the medical field.

Implications of all the available evidence

AI algorithms were beneficial for the diagnosis of tumor metastasis from medical radiology imaging. The methodology and reporting of studies on the AI application in the medical field is often flawed. Normative and rigorous reporting standards should be established to enable the results to be more credible.

captioning, automatic speech recognition, image recognition, natural language processing, drug discovery and bioinformatics [15−19]. Over the past few decades, due to the progress of high-throughput technologies, biomedical data like genome sequences and medical images has experienced explosive growth [20]. With the promising performance of AI in big data and image processing [21,22], more and more people anticipate similar success in the medical field, especially in medical imaging. AI can automatically detect details in medical images, and thus make a quantitative assessment rather than the subjective visual assessment by clinicians. Moreover, human experts may leave out some small metastases, resulting in a missed diagnosis [23−25].

Considering high expectations and demands for AI diagnosis tools in the clinical practice, it is time to review the evidence supporting AI-based diagnosis systematically. In this systematic review and meta-analysis, we were the first to evaluate the diagnostic performance of AI algorithms in tumor metastasis from medical radiology imaging, aiming to guide clinical practice.

2. Methods

2.1. Search strategy and selection criteria

In this systematic review and meta-analysis, we searched for studies that developed or validated an AI model for the diagnosis of tumor metastasis (LNM and DM) from medical radiology imaging. We searched PubMed and Web of Science for studies published from January 1, 1997, to January 30, 2020, with no restrictions on regions, languages, or publication types. A major milestone that happened in 1997 may explain why this starting time was chosen. In 1997, IBM's "Deep Blue" computer defeated the world chess champion Kasparov. After that, artificial intelligence began its positive development. [26] Full search terms and search strategies are provided in the Appendix Section 1.

Reviewers (QZ and LY) screened titles and abstracts of the search results. Uncertainties about inclusion were resolved by the other reviewer (BZ). Studies were included if they evaluated an AI model for the diagnosis of tumor metastasis from medical images with all forms of diagnostic outcomes, such as accuracy, precision, Dice-ratio and recall, etc.. There were no limits on the participants, the type of tumor metastasis, or the intended context for using the model. For the study reference standard to identify whether there is the presence of metastasis, we accepted clinical notes, expert opinion or consensus, and histopathology or laboratory testing.

Giving for radiology images were most widely used in clinical practice to diagnose tumor metastasis, we excluded studies that used histopathology images or medical wave-form data and those focused on the region segmentation of interest to make our study more consistent. We extracted binary diagnosis accuracy data, so ternary diagnosis outcomes were excluded because it had some difference when constructing contingency tables by binary outcomes. Studies that used pre-treatment images to predict conditions of lymph nodes after treatment (e.g. radiotherapy and chemotherapy) were not included because our focus is "diagnosis" other than "prediction". Studies based on animals or nonhuman samples or those presented duplicate data were also excluded.

This systematic review was done following the recommendations of the PRISMA statement [27]. The research question was formulated according to previously published recommendations for systematic reviews of prediction models (CHARMS checklist) [28].

2.2. Data collection

Three reviewers (QZ, LY and JL) extracted data independently using a predefined data extraction sheet, and uncertainties were resolved by another reviewer (BZ). We extracted binary diagnosis accuracy data and constructed contingency tables, which included true-positive (TP), false-positive (FP), true-negative (TN), and false-negative (FN) results if the study provided enough information. Sensitivity and specificity results were calculated from contingency tables.

To evaluate the performance of the AI model, we conducted a meta-analysis from studies providing enough information to construct contingency tables. If a study provided several contingency tables for different algorithms or primary tumors, we treated them as independent items.

The quality of the included studies was evaluated by the reviewers (QZ and KG) and conformed to the revised version of the Quality Assessment of Diagnostic Accuracy Studies (QUADAS) [29].

2.3. Statistical analysis

Receiver operating characteristic (ROC) curves were constructed to evaluate the accuracy of the AI model. The ROC figures provide average sensitivity and specificity across included studies with a 95% confidence interval (CI) of the summary operating point. The ROC figures also provide the 95% prediction region representing the confidence intervals for forecasts of sensitivity and specificity in a future study. Areas under the ROC curve (AUCs) with 95% CI were also calculated. Odds ratio (OR) and 95% CI for each study was calculated to estimate the performance of the AI algorithms.

We calculated heterogeneity between studies using the χ^2 test (threshold $P = 0.1$), which was quantified using the I^2 statistic. We also conducted the subgroup analysis and regression analysis to identify the sources of heterogeneity. Random effects models were used during the process. P value of 0.05 or less was considered to indicate a statistically significant difference.

Two separate analyses were performed according to different algorithms and whether studies were externally validated. Following its development, we divided AI algorithms into ML algorithms (ANN, KNN, SVM, RF, logistic regression and decision tree) and DL algorithms (CNN, DNN and DCNN). External validation means studies were validated by out-of-sample dataset.

To compare diagnostic performance between AI algorithms and health-care professionals, we did another separate analysis for studies providing contingency tables for both health-care professionals and AI algorithm using the same sample. We evaluated the quality of included studies according to QUADAS-2 by RevMan (Version 5.3). Stata (Version 15.0) was used in the ROC curves, the calculation of AUC, subgroup analysis, Deeks' Funnel Plot Asymmetry Test and forest plots. Data analysis was performed by BZ. This study is registered with PROSPERO, CRD42020172924.

2.4. Role of the funding source

3. Results

Fig. 1 summarized our literature search for eligible studies. Our search identified 2620 records, of which 1991 were screened after removing 629 duplicates. 1898 articles were excluded as they did not meet the inclusion criteria. 93 full-text articles were assessed for eligibility and 24 articles were excluded when scanning the full text. As a result, 69 studies were included in the systematic review. Among the 69 studies, 34 studies provided enough information to construct contingency tables and calculate test performance parameters, and were therefore included in the meta-analysis.

These 69 studies described 72 patient cohorts. In these studies, target conditions were divided into LNM (45 studies) and DM (26 studies) (2 studies involved both LNM and DM), which included bone metastasis (13 studies), brain metastasis (3 studies), liver metastasis (4 studies), lung metastasis (2 studies) and others (4 studies). Primary tumors comprised breast cancer (10 studies), head and neck cancer (9 studies), gastric cancer (7 studies), lung cancer (6 studies), colorectal cancer (5 studies), prostate cancer (3 studies) and other primary tumors (6 studies). Thirteen studies did not report this. In addition, 10 studies contained several different primary tumors. Study characteristics are shown in Tables 1, 2 and 3. All included studies used retrospective data and were not open-access. Seven studies excluded low-quality images which meant that the location and size of the lesion on the images did not match that seen at pathologic examination or one or two of the most representative images were selected for each patient, while 62 studies did not report this. Comparison between AI models and health-care professionals by the same test set was only provided in 8 studies. As for the verification of the model, 7 studies collected out-of-sample dataset to do an external validation, and the others were internally validated. Furthermore, different algorithms including DL (23 studies) and ML (34 studies) were included in the systematic review. Four studies used both DL and ML algorithms and 5 studies did not report the detailed types of algorithms.
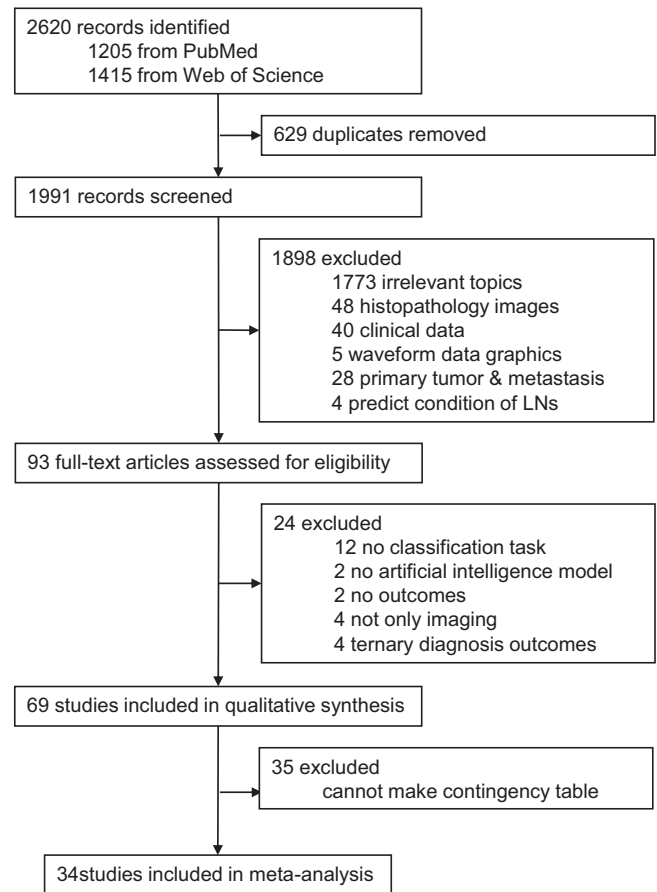

Fig. 1. Study selection.

We accepted all forms of the reference standard for the diagnosis of metastasis. Forty-three studies used histopathology; 21 studies used varying models of expert evaluation; 10 studies used other imaging types to confirm the diagnosis; 7 studies used existing clinical notes; 4 studies used clinical follow-up, and 1 study did not report this. A part of studies applied several different references.

A total of 34 studies and 123 contingency tables were included in the meta-analysis. In these studies, primary tumors included breast cancer (7 studies), head and neck cancer (7 studies), gastrointestinal cancer (4 studies), lung cancer (5 studies) and others (3 studies). 4 studies had several different primary tumors; 4 studies did not report this. There were 25 studies targeting LNM and 10 studies targeting DM (1 study related to both LNM and DM). None of the 8 studies included in the systematic review with comparison between AI models and health-care professionals were excluded in the meta-analysis. After removing 3 from the 7 studies included in the systematic review with external validation because of the lack of contingency tables, only 4 studies were used for the meta-analysis.

In addition, we investigated the international research situation of this subject, finding that the studies mostly concentrated on China, America and Japan, with 31, 11 and 11 studies respectively. Included studies were also widely distributed in South Korea and Europe. South America, Australia and the Middle east had some sporadic distribution as well (Fig. 2).

The quality of studies included in the meta-analysis was assessed by the QUADAS-2 score [29] (Supplementary figure 1). Three and 5 studies showed a high risk respectively for patient selections and reference standards because these studies did not clarify whether enrolled patients were consecutive or use non-histopathology methods as reference standard, which we think were acceptable. So, these studies were not excluded.

Table 1
Participant demographics for the 69 included studies.

First author and year	Participants Inclusion criteria	Exclusion criteria	Patient/Sample	Positive Patients(samples)/ Negative Patients(samples)	Mean age (SD; range), year	Percentage of male participants
Mitsuru Koizumi et al. (2020) [40]	NR	Skeletal metastasis did not meet the criteria of the term 'disseminated'; no skeletal metastasis	54/54	54(NR)/0(NR)	NR	NR
Jing Li et al. (2020) [41]	Patients underwent gastrectomy plus lymph node dissection and were diagnosed gastric adenocarcinomas; patients were scanned with GSI mode; without any local or systematic treatment before CT scans and surgery; with definite postoperative pathologic data.	Invisible lesion on CT images; with a minimum diameter of tumor less than 5 mm insufficient to outline a valid ROI; insufficient stomach distension; poor image quality for post-processing.	204/NR	122(NR)/82(NR)	Training set:59(12;28−81) Test set:59(11;28−74)	Training set:72% Test set:72%
L. Zhang et al. (2020) [42]	NR	NR	51/NR	32(NR)/19(NR)	NR	47%
Li-Qiang Zhou et al. (2020) [43]·*	Patients with histologically confirmed primary breast cancer who underwent surgery; T1 or T2 primary breast cancer with clinically negative LNs and no preoperative therapy; standard preoperative breast US	T3 or T4 stage; physically positive LNs; imaging positive LNs; physically and imaging positive LNs; preoperative therapy; low quality US images	Cohort1: 756/974 Cohort 2:78/81	Training set:343(441)/337(436) Testing set: internal validation:37(49)/39(48) external validation:40(43)/38(38)	Training set:48(NR;24−81) Test set: internal validation:50 (NR;25−82) external validation:46 (NR;30−74)	NR
Endre Grøvik et al. (2020) [44]	The presence of known or possible metastatic disease; no prior surgical or radiation therapy; the availability of all required MRI sequences; patients with ≥1 metastatic lesion	NR	156/156	156(156)/0(0)	63(12;29−92)	33%
Yu Zhao et al. (2019) [45]	Patients with metastatic castration-resistant prostate cancer	NR	193/NR	193(NR)/0(NR)	69.6(7.9;NR)	NR
Jie Xue et al. (2019) [46]	Definitely histopathological results of the primary tumor lesion; patients with only metastatic lesions in brain; with an age over 18 years old; 3D T1 MPRAGE sequence was acquired.	Unqualified imaging quality of 3D T1 MPRAGE; data missing; skull metastases and meningeal metastases	Dataset 1:1201/1201 Dataset 2:231/231 Dataset 3:220/220	Dataset 1:1201(1201)/0(0) Dataset 2:231(231)/0(0) Dataset 3:220(220)/0(0)	Dataset 1:58(18;NR) Dataset 2:60(18;NR) Dataset 3:59(15;NR)	Dataset 1:57% Dataset 2:53% Dataset 3:52%
Bettina Baessler et al. (2019) [47]·*	Patients with retroperitoneally metastasized testicular germ cell tumors prior to post-chemotherapy LN dissection	Absence of contrast-enhanced CT imaging data after chemotherapy and prior to post-chemotherapy LN dissection; insufficient image quality; insufficient matching of histopathology to the individual LNs	80/204 Training set:63/120 Testing set: internal validation:19/23 external validation:41/61	44(107)/36(97) Training set: NR(60)/NR(60) Testing set: NR(15)/NR(8) Validation set: NR(25)/NR(36)	LNM:34(13;NR) N-LNM:36(10;NR)	NR

Table 1 (*Continued*)

First author and year	Participants Inclusion criteria	Exclusion criteria	Patient/Sample	Positive Patients(samples)/ Negative Patients(samples)	Mean age (SD; range), year	Percentage of male participants
Xiaojun Yang et al. (2019) [48]·*	Preoperative contrast-enhanced CT images within 2 weeks before surgery; histologically confirmed primary invasive breast cancer; SLN biopsy (and ALND); pathologically results after operation confirmed SLN metastasis	Neoadjuvant therapy before CT examination and surgery; poor visualization of the tumor for segmentation due to serious artifacts caused by metallic foreign bodies on the breast; tumor was too small to be seen on CT images; incomplete clinicopathological data	348/348 Training set:184/184 Testing set:164/164	Training set:71(71)/113(113) Testing set:63(63)/101(101)	Training set: SLN-P:52(9;NR); SLN—N:50(11;NR) Testing set: SLN-P:50(10;NR); SLN—N:53(10;NR)	NR
Yuan Gao et al. (2019) [49]	NR	No metastatic LNs revealed by CT; with preoperative neoadjuvant radio-chemotherapy; complicated with abdominal infection; pathological grouping different from CT grouping; LN adhesions	602/38,495	NR	62(NR;20−91)	72%
David Coronado-Gutierrez et al. (2019) [50]·*	Positive metastatic nodes by ultrasound-guided FNA or CNB; Negative metastatic nodes determined by histopathology	Surgical biopsy showed positive result after not suspicious nodes in ultrasound exam or negative results of ultrasound-guided FNA or CNB; Patients refused to receive SLNB	127/118	NR(53)/NR(65)	54.6 (NR;26−91)	NR
Yukinori Okada et al. (2019) [51]	NR	NR	56/NR	56(NR)/0(0)	59 (12.7;NR)	0
Jeong Hoon Lee et al. (2019) [52]·*	NR	NR	202/995	NR(348)/NR(647)	NR	NR
Jansen et al. (2019) [53]	NR	Based on visual evaluation, DW-MRI failed to register on the DCE-MR series	111/111	72(NR)/39(NR)	NR	NR
Chuangming Li et al. (2019) [54]·*	Patients had breast cancer confirmed by histology; underwent a DCE-MRI scan before tumor resection or biopsy; received tumor resection and SLNB within 1 week after MRI examination	MRI examination data were incomplete, or image quality was poor	62/62	35(NR)/27(NR)	SLN-P:48.14 (8.35; NR) SLN—N:49.78 (12.53; NR)	NR
M. Dohopolski et al. (2019) [55]	Patients with oropharyngeal squamous cell carcinoma; underwent neck dissections; had preoperative PET and CT imaging	NR	129/543	NR	NR	NR
Yige Peng et al. (2019) [56]·*	NR	No detailed metastases information	48/NR	24(NR)/24(NR)	NR	NR
Qiuxia Feng MD et al. (2019) [57]·*	Definitive diagnosis by histopathology	Neoadjuvant chemotherapy or radiotherapy or endoscopic resection; end-stage disease or severe complications precluding surgery; disease that could not be detected on imaging; poor imaging quality or poor gastric resection	490/NR	279(NR)/211(NR)	61.8(10.4; NR)	Training and validation set: 73% Test set: 77%

Table 1 (*Continued*)

First author and year	Participants Inclusion criteria	Exclusion criteria	Patient/Sample	Positive Patients(samples)/ Negative Patients(samples)	Mean age (SD; range), year	Percentage of male participants
Thoma Schnelldorfer et al. (2019) [58]	Underwent a laparoscopic operation with the initial intent for either resection or palliation of the underlying malignancy; Video recordings of the operation were available	Malignancy originating from esophageal, hepatic and colorectal malignancies	35/35	20(20)/15(15)	67 (NR;44~85)	66%
Samir D. Mehta et al. (2019) [59]*	Underwent CT of the abdomen and pelvis or radiographs of the lumbar spine and DEXA studies; CT studies/ lumbar spine radiographs were performed not more than 1 year prior to the DEXA study	NR	200/NR	45(NR)/155(NR)	Case: 70.5 (NR;63.9~76.7) Control: 62 (NR;53.5~69)	Case: 78% Control: 83%
Yoshiko Ariji, et al. (2019) [60]*	Underwent intravenous contrast enhanced CT and dissection of cervical lymph nodes	NR	45/441	NR(127(/NR(314)	63 (NR;33~95)	53%
Yunpeng Zhou et al. (2019) [61]	Definite lymph node metastasis reported by preoperative imaging	With a history of abdominal pelvic surgery, and pelvic radio-chemotherapy	301/12,060	301(NR)/0(NR)	59.5(NR; NR)	75%
Yu Li et al. (2019) [62]*	Received radical colectomy with lymph node dissection; Patients with colon cancer diagnosis; Patients with no history of previous or coexisting other malignancies; Patients who underwent preoperative enhanced CT for local colon cancer staging and for liver metastasis diagnosis;	Patients who underwent treatment (radiotherapy, chemotherapy or chemoradiotherapy) before the baseline CT examination; Poor image quality; Patients with liver metastasis who did not receive synchronous resection of the primary tumor and liver metastasis	48/NR	24(NR)/24(NR)	LNM: 63.3 (11.21; NR) Non-LNM: 59.71 (13.86; NR)	63%
Zhiguo Zhou et al. (2019) [63]*	NR	NR	129/543	Training set: NR (91)/NR (287) Test set: NR (39)/NR (126)	NR	NR
eMine acar et al. (2019) [64]	Sclerotic lesions >2 cm in patients with at least three sclerotic metastatic lesions; sclerosis areas of the bones that located on the surface of the joint and/or on the surface of the other side of the joint; osteophytes not considered as metastasis.	No bone metastasis; <3 bone metastasis; no sclerotic metastasis; uptake<liver uptake	75/257	NR(153)/NR(104)	69(9; NR)	NR
Fang Hou et al. (2019) [65]*	NR	NR	28/573	Training set: NR (21)/NR (293) Test set: NR (25)/NR (234)	NR	NR
Yoshiko Ariji et al. (2019) [66]*	Oral squamous cell carcinoma; underwent neck dissection; pathology confirms cervical lymph node metastasis	NR	54/143 (LN) 703 (image)	NR (33)/NR (110)	64(NR; NR)	52.94%

Table 1 (*Continued*)

First author and year	Participants Inclusion criteria	Exclusion criteria	Patient/Sample	Positive Patients(samples)/ Negative Patients(samples)	Mean age (SD; range), year	Percentage of male participants
Xiaojuan Xu et al. (2019) [67]	Patients who received standard FIGO surgical staging for endo-metrial cancer between January 2011 and December 2017	Patients without DCE-MRI 2 weeks before surgery; patients with serious MR artifacts and without uniform MR scanner; patients missing clinical characteristics data and endometrial biopsy histological information; patients with any preoperative therapy; patients suffering from other malignant tumor diseases concurrently	200/NR	67(NR)/133(NR)	Training cohort: pN(+):55.7(NR; NR) pN(-):55.7 (NR; NR) Test Cohort: pN(+):57.4(NR; NR) pN(-):51.7(NR'; NR)	NR
Jiaxiu Luo et al. (2018) [68]·*	NR	NR	172/NR	74(NR)/98(NR)	NR	NR
Richard Ha et al. (2018) [69]	NR	NR	275/275	133(133)/142(142)	NR	NR
B.H. Kann et al. (2018) [70]·*	NR	NR	270/653	NR (380)/NR (273)	NR	NR
Jeong Hoon Lee et al. (2018) [71]·*	NR	NR	804/812 cohort1:604/612 cohort2:200/200	Training set: NR (286)/NR 263 Validation set: NR (33)/NR (30) Test set: NR (100)/NR (100)	Training & Validation set:44 (NR;13−84) Test set:55(NR;10−81)	Training & Validation set:30.6% Test set:27%
Yun Lu et al. (2018) [72]	NR	NR	Training set:351/28,080 Test set:414/36,000	Training set:351(28,080)/0(0) Test set: NR	NR	NR
José Raniery Ferreira Junior et al. (2018) [73]·*	NR	No standard contrast-enhanced CT protocol; did not present all clinical data; presented other opacities attached to the tumor	68/NR	LNM: Test:23(NR)/29(NR) Validation set:9(NR)/7(NR) DM: Test:8(NR)/44(NR) Validation set:5(NR)/11(NR)	Test set:66.6(9.1;41−85) Validation set:64.88(9.1;41−79)	Test set:57.7% Validation set:62.5%
Tzu-Yun Lo et al. (2018) [74]	NR	NR	70/75	70(75)/0(0)	NR	NR
Jin Li et al. (2018) [75]	NR	NR	NR/619	Original data: NR(307)/NR(312) augmented data: NR(1535)/NR (1560)	NR	NR
Mohamed Amine Larh-mam et al. (2018) [76]	NR	NR	NR/153	NR (87)/NR (66)	NR	NR
Yan Zhong et al. (2018) [77]·*	Underwent surgical resection and systematic LN dissection according to the American Thoracic Society criteria; had no enlargement of the hilar or mediastinal LNs at CT (enlargement defined as short axis of a node ≥ 10 mm on axis images) and clinical N0; no distal metastasis	IV administration of contrast material; unsatisfactory image quality due to respiratory arti-fact during the examination that may have disturbed fea-ture extraction; and surgical resection not performed within 90 days of thin-section CT	492/492	78(78)/414(414)	61.4(9.7; NR) N-LNM:61.28(9.8; NR) LNM:61.71(9.62; NR)	35% N-LNM:32% LNM:50%
Wang, H et al. (2017) [78]·*	NR	NR	168/1397	NR (127)/NR (1270)	61(NR;38−81)	54%
Mitsuru Koizumi et al. (2017) [79]·*	NR	NR	265/265	124(124)/101(101)	NR	NR
Juan Wang et al. (2017) [80]	NR	NR	26/NR	26(NR)/0(NR)	58(14; NR)	54%

Table 1 (*Continued*)

First author and year	Participants Inclusion criteria	Exclusion criteria	Patient/Sample	Positive Patients(samples)/ Negative Patients(samples)	Mean age (SD; range), year	Percentage of male participants
Zhi-Long Wang et al. (2017) [81]	NR	Pathologically proven adenocarcinoma, small cell carcinoma, mixed cancer, or other diseases; other preoperative therapies simultaneously; esophageal multiple primary carcinoma; death within 30 days after surgery; enhanced CT data before preoperative chemotherapy not obtained or images not interpretable; non-suitability for radical esophagectomy	131/NR	51(NR)/80(NR)	58(NR;42−75)	77.90%
Tuan D. Pham et al. (2017) [82]·*	Biopsy-proven primary lung malignancy with pathological mediastinal nodal staging;	Patients with nodal biopsy more than three months from CT	148/NR	Test set: NR (133)/NR (138)	69.4(NR;36−84)	63%
Qi Zhang et al. (2017) [83]·*	Underwent axilla conventional US and RTE simultaneously	Take neoadjuvant therapy before SLNB or ALND	158/161	NR (92)/NR (69)	55.2(5.2;21−81)	NR
Yu-wen Wang et al. (2016) [84]·*	NR	A relatively large (minimal axial diameter up to 10 mm) necrotic node, which did not promptly respond to RT	Stage I: 335/663 Stage II: 210/410	Stage I: NR (337)/NR (326); Stage II: NR (211)/NR (199)	NR	NR
Ali Aslantas et al. (2016) [85]·*	NR	NR	60/130	39(34)/21(96)	57(NR;30−87)	60%
Aneta Chmielewski et al. (2015) [86]·*	Underwent surgical treatment for invasive breast cancer with axillary lymph node evaluation	NR	77/105	NR (24)/NR (81)	NR	0
Mitsuru Koizumi et al. (2015) [87]·*	NR	NR	426/NR	152(NR)/274(NR)	NR	NR
Mitsuru Koizumi et al. (2015) [88]	NR	Patient showing segmentation error on BONENAVI version 2	394/NR	142(NR)/252(NR)	NR	NR
Nesrine Trabelsi et al. (2015) [89]	NR	NR	11/NR	11(NR)/0(NR)	NR	NR
Xuan Gao et al. (2015) [90]	NR	NR	132/768	NR	NR	60.60%
Osamu Tokuda, et al. (2014) [91]·*	NR	Benign conditions; did not undergo follow-up examinations; younger than 20 years of age	406/3248	90(235)/316(3013) Prostatic cancer: NR(104)/NR(464); Breast cancer: NR(42)/NR(830); Males with other cancer: NR(56)/NR(1168); Females with other cancers: NR(33)/NR(551)	66(NR;27−92)	55%
Ari Seff et al. (2014) [92]	NR	NR	Mediastinal LN:90/389(LN) Abdominal:86/595(LN)	Mediastinal LN:NR(960Candidates)/NR(3208Candidates) Abdominal: NR(1005Candidates)/NR(3484Candidates)	NR	NR
Zhi-Guo Zhou et al. (2013) [93]·*	NR	NR	175/175	134(NR)/41(NR)	59.8(NR;30−85)	71%
Seungwook Yang et al. (2013) [94]·*	NR	Excessive motion artifacts	26/90	Test Set: black-blood:26(53)/0(443); MP-RAGE:26(53)/0(5788)	NR	NR

Table 1 (*Continued*)

First author and year	Participants Inclusion criteria	Exclusion criteria	Patient/Sample	Positive Patients(samples)/ Negative Patients(samples)	Mean age (SD; range), year	Percentage of male participants
Jianfei Liu et al. (2013) [95]	NR	NR	50/NR	Training set: NR; Test set:44 (102)/NR	NR	NR
Yoshihiko Nakamura et al. (2013) [96]	NR	NR	28/NR	28(95)/0(NR)`	NR	NR
Chuan-Yu Chang et al. (2013) [97]	NR	NR	6/177	All positive	NR	NR
Johannes Feulner et al. (2013) [98]	NR	NR	54/1086	NR(289)/NR(NR)	NR	NR
Chao Li et al. (2012) [99]	NR	NR	38/NR	27(NR)/11(NR)	NR	NR
Hongmin Cai et al. (2012) [100]	NR	NR	228/NR	NR	58(NR;19−86)	61%
Shao-Jer Chen et al. (2012) [101]	NR	NR	37/149	13(55)/24(94)	LN:64(10;44−77) N-LN:47(13;15−68)	LN:61.5% N-LN:41.7%
Xiao-Peng Zhang et al. (2011) [102]·*	Patients received radical gastrectomy and D2 lymph nodes dissection; Preoperatively examined with multi-detector row CT; Confirmed as gastric cancer by postoperative histopathology	Received preoperative neoadjuvant therapy; Distant metastasis was found in the preoperative examination or in the operation	175/NR	134(NR)/41(NR)	59.8 (NR;30~85)	71%
Matthias Dietzel et al. (2010) [103]	Invasive breast lesions with histopathological verification after bMRI	With a history of breast biopsy/interventions (surgical or minimally invasive) and chemotherapy/radiation therapy up to 12 months before bMRI; Histopathological grading not possible	194/NR	97(NR)/97(NR)	60.6 (12.1; 25~87)	NR
May Sadik et al. (2008) [104]·*	Underwent whole-body bone scintigraphy with a dual-detector r-camera; Patients with a complete set of technically sufficient images; At least 1 yr follow-up bone scan	Patients with a urine catheter, large bladder, sternotomy or fracture that could be misleading for the CAD system	NR/869	NR(297)/NR(572)	Training set: 66 (NR;25~92) Test set: 65 (NR;43~86)	Training: 65% Test: 69% All: 62%
Junji Shiraishi et al. (2008) [105]	NR	NR	97/103	NR(26);NR(77)	NR	NR
Junhua Zhang et al. (2008) [106]·*	NR	NR	112/210	NR(114)/NR(96)	53 (17;17~81)	NR
Rie Tagaya et al. (2008) [107]·*	NR	NR	91/91	Training set:6(6)/3(3) Test set:60(60)/22(22)	NR	NR
K. Marten et al. (2004) [108]	Patients with pulmonary metastasis; undergoing clinical staging and follow-up CT examinations of the chest	NR	20/135	20(NR)/0(NR)	62.4(NR;NR)	NR

Abbreviation: NR=not reported. CT=computed tomography. GSI=Gemstone spectral imaging. LN= Lymph node. US= ultrasound. 3D-T1-MPRAGE images=Three-dimensional T1 magnetization prepared rapid acquisition gradient echo. SLN= sentinel lymph node. ALND= axillary lymph node dissection. FDG-PET/CT= fluoro-deoxy glucose positron emission tomography with CT. MRI= magnetic resonance imaging. FNA= fine needle aspiration. CNB= core needle biopsy. DW-MRI= diffusion-weighted magnetic resonance imaging. DCE-MR= contrast-enhanced magnetic resonance imaging. OPSCC= oropharyngeal squamous cell carcinoma. DEXA=Dual-energy X-ray absorptiometry. HNC=head and neck cancer. DCE-MRI= dynamic contrast enhanced MRI. FIGO=International Federation of Gynecology and Obstetrics. RTE=real-time elastography. NPC=nasopharyngeal carcinoma. CAD=computer-assisted diagnosis.

* 34 studies included in the meta-analysis.

Table 2
Model training and validation for the 69 included studies.

First author and year	Metastasis type	Target condition	Primary tumor	Reference standard	Type of internal validation	External validation
Mitsuru Koizumi et al. (2020) [40]	DM	Disseminated skeletal metastasis	prostate cancer(n = 12), GC= (n = 12), breast cancers (n = 15), miscellaneous cancers (n = 10)	Expert consensus	NR	YES
Jing Li et al. (2020) [41]	LNM	LNM in GC	GC	Histopathology; follow up	Resampling method	NO
L. Zhang et al. (2020) [42]	DM	Lung metastasis in STS	STS	Histopathology	Random split sample validation	NO
Li-Qiang Zhou et al. (2020) [43]·*	LNM	Clinically negative axillary lymph node metastasis in primary breast cancer	Breast cancer	Histopathology	NR	YES
Endre Grøvik et al. (2020) [44]	DM	Detection and Segmentation of Brain Metastases	Lung (n = 99), breast (n = 33), melanoma (n = 7), genitourinary (n = 7), gastrointestinal (n = 5), and miscellaneous-cancers (n = 5)	Expert consensus	NR	NO
Yu Zhao et al. (2019) [45]	DM& LNM	Bone metastasis, lymph node metastasis in prostate cancer	Metastatic castration-resistant prostate cancer	Expert consensus	NR	NO
Jie Xue et al. (2019) [46]	DM	Detection and Segmentation of Brain Metastases	Lung, Breast, Kidney, Other organs (rectum, colon, melanoma, ovary and liver)	Expert consensus	Resampling method	NO
Bettina Baessler et al. (2019) [47]·*	LNM	LNM in NSTGCT patients	NSTGCT	Histopathology	Resampling method	NO
Xiaojun Yang et al. (2019) [48]·*	LNM	SLNM in Breast Cancer	Breast cancer	Histopathology	Resampling method	NO
Yuan Gao et al. (2019) [49]	LNM	PGMLNs in GC	GC	Histopathology; expert consensus	Resampling method	NO
David Coronado-Gutierrez et al. (2019) [50]·*	LNM	Metastasis in the axillary lymph node	Breast cancer	Histopathology	Resampling method	NO
Yukinori Okada et al. (2019) [51]	DM	Bone metastasis	Breast cancer	Based on CT, MRI and clinical findings: expert consensus	NR	NR
Jeong Hoon Lee et al. (2019) [52]·*	LNM	Metastasis in the cervical lymph node	Thyroid cancer	Histopathology by FNA and/or surgery	Random split sample validation	NO
Jansen et al. (2019) [53]	DM	Liver metastasis	NR	Expert consensus	NR	NO
Chuangming Li et al. (2019) [54]·*	LNM	Sentinel lymph node metastasis	Breast cancer	Histopathology; expert consensus	NR	NO
M. Dohopolski et al. (2019) [55]	LNM	Small Lymph node metastasis	Oropharyngeal squamous cell carcinoma	Histopathology	NR	NO
Yige Peng et al. (2019) [56]·*	DM	Distant metastasis in STS	STS	Biopsy or CT and/or PET images	NR	NO
Qiuxia Feng MD et al. (2019) [57]·*	LNM	LNM in GC	GC	Histopathology	NR	NO
Thoma Schnelldorfer et al. (2019) [58]	DM	Distinguish metastasis in the peritoneal from the benign lesions	Gastric adenocarcinoma: 19. Pancreatic adenocarcinoma: 11; Gallbladder carcinoma: 2. Metastatic pancreatic neuroendocrine tumor, jejunal adenocarcinoma, ampullary adenocarcinoma: 1 each	Histopathology	NR	NO
Samir D. Mehta et al. (2019) [59]·*	DM	Osteoblastic metastases involving one or more vertebral bodies from L1 to L4	NR	Clinical notes	Random split sample validation	NO
Yoshiko Ariji, et al. (2019) [60]·*	LNM	Metastasis in the cervical lymph node	Oral cancer	Histopathology	Resampling method	NO
Yunpeng Zhou et al. (2019) [61]	LNM	LNM in rectal cancer	Rectal cancer	Expert consensus	NR	NO
Yu Li et al. (2019) [62]·*	DM	Metastasis in the liver of the preoperative CT	Colon cancer	Histopathology	Resampling method	NO
Zhiguo Zhou et al. (2019) [63]·*	LNM	LNM in HNC	HNC	Histopathology	NR	NO

Table 2 (*Continued*)

First author and year	Metastasis type	Target condition	Primary tumor	Reference standard	Type of internal validation	External validation
eMine acar et al. (2019) [64]	DM	Differentiating metastatic and completely responded sclerotic bone lesion in prostate cancer	Prostate cancer	Expert consensus	Resampling method	NO
Fang Hou et al. (2019) [65]·*	LNM	LNM	NR	Histopathology	NR	NO
Yoshiko Ariji et al. (2019) [66]·*	LNM	LNM in Oral squamous cell carcinoma	Oral squamous cell carcinoma	Histopathology	NR	NO
Xiaojuan Xu et al. (2019) [67]	LNM	LNM in EC	EC	Histopathology	NR	NO
Jiaxiu Luo et al. (2018) [68]·*	LNM	SLNM in breast cancer	Breast cancer	Histopathology	NR	NO
Richard Ha et al. (2018) [69]	LNM	LNM in breast cancer	Breast cancer	Biopsy; follow up	Resampling method	NO
B.H. Kann et al. (2018) [70]·*	LNM	LNM in HNC	HNC	Histopathology	Resampling method	NO
Jeong Hoon Lee et al. (2018) [71]·*	LNM	LNM in thyroid tumor	Thyroid tumor	FNA and/or laboratory tests	Random split sample validation	NO
Yun Lu et al. (2018) [72]	LNM	Pelvis LNM in rectal cancer	Rectal cancer	Expert consensus	Random split sample validation	YES
José Raniery Ferreira Junior et al. (2018) [73]·*	DM& LNM	LNM and distant metastasis in lung cancer	Lung cancer	Clinical notes	Resampling method	NO
Tzu-Yun Lo et al. (2018) [74]	LNM	LNM in HNC	HNC	Clinical notes	Resampling method	NO
Jin Li et al. (2018) [75]	LNM	LNM in Colorectal Cancer	Colorectal Cancer	Expert consensus	NR	NO
Mohamed Amine Larhmam et al. (2018) [76]	DM	Spine metastasis	NR	Single expert	Resampling method	NO
Yan Zhong et al. (2018) [77]·*	LNM	Occult mediastinal LNM of lung adenocarcinoma	Lung adenocarcinoma	Histopathology	Resampling method	NO
Wang, H et al. (2017) [78]·*	LNM	Mediastinal LNM of non-small cell lung cancer	Non-small cell lung cancer	Histopathology	Resampling method	NO
Mitsuru Koizumi et al. (2017) [79]·*	DM	Skeletal metastasis in prostate cancer	Prostate cancer	BS&CT expert consensus; follow up; and/or biopsy	NR	YES
Juan Wang et al. (2017) [80]	DM	Spinal metastasis	15 lung, 5 thyroid, two liver, 1 breast, 1 prostate, 1 esopha-gus, 1 urinary tract	Biopsy	Resampling method	NO
Zhi-Long Wang et al. (2017) [81]	LNM	LNM in esophageal cancer with preoperative chemotherapy	Esophageal cancer	Postoperative pathological results	Random split sample validation	NO
Tuan D. Pham et al. (2017) [82]·*	LNM	Mediastinal lymph nodes in lung Cancer	Lung cancer	Histopathology	Resampling method	NO
Qi Zhang et al. (2017) [83]·*	LNM	Axillary lymph node metastasis in breast cancer	Breast cancer	Histopathology	Resampling method	NO
Yu-wen Wang et al. (2016) [84]·*	LNM	Metastasis in the retropharyng-eal lymph nodes	NPC	MRI follow-up	Random split sample validation	NO
Ali Aslantas et al. (2016) [85]·*	DM	Bone metastatic	Chest, prostate, lung cancers	Single expert (laboratory tests, and other accessible radio-graphic images)	Resampling method	NO
Aneta Chmielewski et al. (2015) [86]·*	LNM	Axillary lymph node metastasis in breast cancer patients	Breast cancer	Imaging-pathology gold stand-ards: FNA, biopsy, LND, normal image with long term follow-up	Resampling method	NO
Mitsuru Koizumi et al. (2015) [87]·*	DM	Metastasis in bone	Prostate cancer, lung cancer, breast cancer, and other cancers	Radiology (CT, MR or PET/CT), follow-up scan and patients' clinical course	NR	YES
Mitsuru Koizumi et al. (2015) [88]	DM	Metastasis in bone	Prostate cancer, lung cancer, breast cancer, and other cancers	Radiology (CT, MR or PET/CT), follow-up scan and patients' clinical course	NR	YES
Nesrine Trabelsi et al. (2015) [89]	DM	Metastasis in liver	NR	NR	NR	NO
Xuan Gao et al. (2015) [90]	LNM	Mediastinal lymph nodes in lung cancer	Lung cancer	Histopathology	Random split sample validation	NO

Table 2 (*Continued*)

First author and year	Metastasis type	Target condition	Primary tumor	Reference standard	Type of internal validation	External validation
Osamu Tokuda, et al. (2014) [91]*	DM	Bone metastasis	Prostatic cancer (*N* = 71), breast cancer (*N* = 109), other cancers (*N* = 226)	All bone-scan images, including the follow-up scans, expert consensus; laboratory tests; (OR) biopsy	NR	YES
Ari Seff et al. (2014) [92]	LNM	LNM	NR	Expert consensus	Resampling method	NO
Zhi-Guo Zhou et al. (2013) [93]*	LNM	LNM in GC	GC	Surgery and histopathology	Resampling method	NO
Seungwook Yang et al. (2013) [94]*	DM	Brain metastases	NR	Single expert	NR	NO
Jianfei Liu et al. (2013) [95]	DM	Ovarian Cancer Metastases	Ovarian Cancer	Single expert	NR	NO
Yoshihiko Nakamura et al. (2013) [96]	LNM	Abdominal Lymph Node	5 colorectal; 23 stomach cancer	26cases: single expert 2 cases: experts consensus using a particular medical image	Resampling method	NO
Chuan-Yu Chang et al. (2013) [97]	LNM	LNM	NR	Histopathology	NR	NO
Johannes Feulner et al. (2013) [98]	LNM	Mediastinal lymph nodes	NR	Single expert	Resampling method	NO
Chao Li et al. (2012) [99]	LNM	LNM in GC	GC	Histopathology	NR	NO
Hongmin Cai et al. (2012) [100]	LNM	Regional LNM	Rectal cancer	Histopathology	Resampling method	NO
Shao-Jer Chen et al. (2012) [101]	LNM	LNM	NR	Histopathology; follow up	Resampling method	NO
Xiao-Peng Zhang et al. (2011) [102]*	LNM	LNM in GC	GC	Histopathology	Resampling method	NO
Matthias Dietzel et al. (2010) [103]	LNM	Metastasis to the ipsilateral axilla lymph node	Breast cancer	Surgicopathology	Random split sample validation	NO
May Sadik et al. (2008) [104]*	DM	Metastasis to bone	Testing: Breast/prostate cancer	Training: Clinical reports and the bone scan images Testing: Final clinical assessments made by the same experienced physician	NR	NO
Junji Shiraishi et al. (2008) [105]	DM	Metastasis to the liver	NR	Biopsy or surgical specimens	NR	NO
Junhua Zhang et al. (2008) [106]*	LNM	Metastasis to the cervical lymph nodes	NR	Histopathology	Resampling method	NO
Rie Tagaya et al. (2008) [107]*	LNM	Diagnosis of LNM by B-Mode Images from Convex-Type Echobronchoscopy	66 lung cancer,25sarcoidosis	Histopathology or cytologic testing	NR	NO
K. Marten et al. (2004) [108]	DM	Pulmonary nodules	NR	Expert consensus	NR	NO

Characteristics only be described in 1 or 2 studies are classified to others.

Abbreviation: NR=not reported. LNM=Lymph node metastasis. DM= distant metastasis. BS=bone scintigraphy. GC=gastric cancers. STS=soft-tissue sarcoma. NSTGCT= Non-seminomatous testicular germ cell tumor. PGMLNs= peri-gastric metastatic lymph nodes. EC=Endometrial cancer. FNA=fine needle aspiration.

* 34 studies included in the meta-analysis.

Table 3

Indicator, algorithm, and data source for the 69 included studies.

First author and year	Indicator definition				Algorithm			Data source			
	Method for predictor measurement	Exclusion of poor-quality imaging	Heatmap provided	Extracted features	Algorithm architecture name	Algorithm architecture	Transfer learning applied	Source of data	Number of images for training/testing)	Data range	Open access data
Mitsuru Koizumi et al. (2020) [40]	BS	NR	NR	NO	NR	ANN	NR	Retrospective clinical data from cancer institute hospital, Tokyo, Japan	NR/54	2013.1−2019.8	NO
Jing Li et al. (2020) [41]	dual-energy CT	YES	NR	YES	DCNNs; ANN; Ksvm	CNN; ANN; SVM	NR	Retrospective cohort	136/68	2012.1−2018.11	NO
L. Zhang et al. (2020) [42]	MRI, CT	NR	NR	NO	Inception V3	CNN; Inception	YES	Data collected from Cancer Imaging Archive	25/15	NR	YES
Li-Qiang Zhou et al. (2020) [43]*	US image	YES	YES	NO	Inception V3; Inception-ResNet V2; ResNet-101	CNN; Inception; Residual Network	NR	Cohort 1: retrospective cohort collected from Tongji Hospital; Cohort 2: retrospective cohort collected from Hubei Cancer Hospital (Hubei, China) 1:2016.5−2018.10; Cohort 2:2018.10−2019.4	877/97(internal test) +81 (external test) NO	Cohort	NO
Endre Grøvik et al. (2020) [44]	Multisequence MRI	NR	YES	NO	GoogLeNet	CNN	NR	Retrospective cohort	100/51	2016.6−2018.6	NO
Yu Zhao et al. (2019) [45]	PSMA PET/CT, CT	NR	NR	NR	triple combing 2.5D U-NET	CNN	NR	Retrospective cohort from medical centers of Technical University of Munich, University of Munich and University of Bern	130/63	NR	NR
Jie Xue et al. (2019) [46]	3D-T1-MPRAGE images	YES	NR	NO	3D CNN	CNN	NR	Dataset 1: Retrospective clinical data from the Shandong Provincial Hospital Affiliated to Shandong University; Dataset 2: Retrospective clinical data from the Affiliated Hospital of Qingdao University Medical College; Dataset 3: Retrospective clinical data from the Second Hospital of Shandong University 1:2016.10−2019.5 Dataset 2:2017.8−2019.3 Dataset 3:2017.4−2019.4	1201/451 NO	Dataset	NO
Bettina Baessler et al. (2019) [47]*	CT	YES	NR	YES	logistic regression	logistic regression	NR	Retrospective cohort	120/23(internal test)+61 (external test)	2008−2017	NO
Xiaojun Yang et al. (2019) [48]*	CT	YES	NR	YES	CNN-F; multivariable logistic regression	CNN; logistic regression	YES	Retrospective cohort	184/164	2016.1−2018.11	NO
Yuan Gao et al. (2019) [49]	CT	YES	NR	YES	FR-CNN	CNN	NR	Cohort 1: retrospective cohort collected from Tongji Hospital Cohort 2: retrospective cohort collected from Hubei Cancer Hospital (Hubei, China)	32,495/6000	2011.1−2018.5	No
David Coronado-Gutierrez et al. (2019) [50]*	US	YES	NR	YES	CNN; VGG-M	VGG	NR	Retrospective cohort	NR/NR	2015.4−2018.8	NO

(continued on next page)

Table 3 (Continued)

First author and year	Indicator definition				Algorithm			Data source			
	Method for predictor measurement	Exclusion of poor-quality imaging	Heatmap provided	Extracted features	Algorithm architecture name	Algorithm architecture	Transfer learning applied	Source of data	Number of images for training/testing	Data range	Open access data
Yukinori Okada et al. (2019) [51]	BS	NR	NR	NO	NR	CNN	NR	Retrospective cohort	NR/NR	2012.1–2014.11	NO
Jeong Hoon Lee et al. (2019) [52]*	CT(Axial)	NR	YES	NO	VGG16; VGG19; Inception; Inception V3; InceptionRes-NetV2; D3nse-Net121; DenseNet169; ResNet	CNN; VGG; Inception; Residual Network	NR	Retrospective cohort	891/104	2017.7–2018.1	NO
Jansen et al. (2019) [53]	Contrast-enhanced MRI, diffusion-weighted MRI	NR	NR	NR	NR	CNN-F	NR	Retrospective cohort from University Medical Center Utrecht, The Netherlands	55 /17	2015.2–2018.2	NO
Chuangming Li et al. (2019) [54]*	Contrast-enhanced MRI	YES	NR	YES	Logistic regression; SVM; XGBoost	NR	NR	Clinical data from the Second Affiliated Hospital of Chongqing Medical University, China	49/13	2013.3–2018.12	YES
M. Dohopolski et al. (2019) [55]	PET, CT	NR	NR	NR	AlexNet-like, UNET	CNN	NR	NR	4074/54	NR	NR
Yige Peng et al. (2019) [56]*	PET-CT	NR	NR	YES	3D deep multi-modality collaborative learning	CNN	NR	Public PET-CT dataset of STS patients	NR/NR	NR	YES
Qiuxia Feng MD et al. (2019) [57]*	CT	YES	NR	YES	NR	NR	NR	Retrospective cohort from the First Affiliated Hospital with Nanjing Medical University, Nanjing, China	326/164	2014.1–2016.12	NO
Thoma Schnelldorfer et al. (2019) [58]	Laparoscopy	NR	NR	NR	DNN	Deep neural network	NR	Retrospective cohort	NR/NR		
Samir D. Mehta et al. (2019) [59]*	Dual X-ray absorptiometry	NR	NR	NR	Radom forest algorithm; SVM	Radom forest algorithm; SVM	NR	2014.1.1–2017.9.30 Retrospective cohort	NO 160/40		
Yoshiko Ariji, et al. (2019) [60]*	CT (Contrast enhanced, axial)	NR	NR	NR	AlexNet	AlexNet	NR	2010.1.1–2018.8.31 Retrospective cohort	NO 353/88	2007–2015	NO
Yunpeng Zhou et al. (2019) [61]*	High-resolution MRI	NR	NR	NR	Faster region-based CNN	FRCNN	NO	Retrospective cohort	Patients: 201/100 Images: 12,060/6030	2016.7–2017.12	NO
Yu Li et al. (2019) [62]*	CT	YES	NR	YES	SVM	SVM	NR	Retrospective cohort	240/240	2015.10–2018.7	NO
Zhiguo Zhou et al. (2019) [63]*	CT; PET; PEC&CT	NR	NR	YES	MO; CNN; AutoMO	SVM; CNN	NR	Retrospective cohort from the University of Texas Southwestern Medical Center	378/165	2009–2018	NO
eMine acar et al. (2019) [64]	68Ga-PSMA PET/CT	NR	NR	YES	Decision tree; discriminant analysis; SVM; KNN; BP-ANN	Decision tree; discriminant analysis; SVM; KNN, ANN	NR	Retrospective cohort	153/104	2017.1–2018.11	NO
Fang Hou et al. (2019) [65]*	OCT	NR	NR	YES	ANN	ANN	NR	Retrospective cohort from Department of Head and neck Tumor, Tianjin Medical University Cancer Institute and Hospital, China	314/259	NR	NO
Yoshiko Ariji et al. (2019) [66]*	CT	NR	NR	NR	AlexNet	CNN	NR	Retrospective cohort from Aichi-Gakuin University School of Dentistry, Nagoya, Japan	562/141	2017–2018	NR

Table 3 (*Continued*)

First author and year	Indicator definition				Algorithm			Data source			
	Method for predictor measurement	Exclusion of poor-quality imaging	Heatmap provided	Extracted features	Algorithm architecture name	Algorithm architecture	Transfer learning applied	Source of data	Number of images for training/testing	Data range	Open access data
Xiaojuan Xu et al. (2019) [67]	Contrast-enhanced-MRI	NR	YES	YES	NR	NR	NR	Retrospective cohort from National Cancer Center, Chinese Academy of Medical Sciences and Peking Union Medical College, Beijing, China	140/60	2011.1–2017.12	NO
Jiaxiu Luo et al. (2018) [68]*	diffusion-weighted MRI	NR	NR	YES	CNN; SVM	SVM; CNN	NR	Retrospective cohort	122/50	2014.3–2016.6	NO
Richard Ha et al. (2018) [69]	MRI	NR	NO	NO	CNN; VGG-16	CNN; VGG	NR	Retrospective cohort	NR/NR	2013.1–2016.6	NO
B.H. Kann et al. (2018) [70]*	CT	NR	NR	NO	DCNNs	CNN	NR	Retrospective cohort	522/131	2013–2017	NO
Jeong Hoon Lee et al. (2018) [71]*	US	NR	YES	NO	VGG-Class Activation Map;CNN-GAP	CNN; VGG	NR	Retrospective cohort	612/200	cohort1:2008.1–2015.11 cohort2:2016.1–2016.11	NO
Yun Lu et al. (2018) [72]	MRI	NR	NR	NO	FR-CNN; VGG16	CNN; VGG	YES	Training set: Retrospective cohort from Affiliated Hospital of Qingdao University; Test set: Retrospective cohort from 6 Chinese Medical Centers	28,080/36,000	cohort1:2011.9–2018.10 cohort2:NR	NO
José Raniery Ferreira Junior et al. (2018) [73]*	CT	YES	YES	YES	NB; KNN; RBF; ANN	KNN; ANN	NR	Retrospective cohort	52/16	NR	NO
Tzu-Yun Lo et al. (2018) [74]	CT	NR	NR	YES	SVM	SVM	NR	Retrospective cohort from Taipei Veterans General Hospital of Taiwan	NR/NR	NR	NO
Jin Li et al. (2018) [75]	MRI	NR	NR	NO	Inception-v3	CNN	YES	Data collected from Harbin Medical University Cancer Hospital	NR/NR	NR	NO
Mohamed Amine Larhmam et al. (2018) [76]	MRI	NR	NR	YES	SVM	SVM	NR	NR	NR/NR	NR	NR
Yan Zhong et al. (2018) [77]*	CT	YES	NR	YES	RBF; SVM	SVM	NR	Retrospective cohort	NR/NR	2013.1–2016.9	NO
Wang, H et al. (2017) [78]*	18F-FDG PET/CT	NR	NO	YES	Random forest; AdaBoost; SVM; BP-ANN	Random forest; AdaBoost; SVM; BP-ANN	NR	Retrospective cohort from Cancer Hospital Affiliated to Harbin Medical University	200/1197	2009.6–2014.9	NO
Mitsuru Koizumi et al. (2017) [79]*	BS	NR	NR	NO	BONENAVI	ANN	NR	NR	NR/NR	2013.2–2017.1	NO
Juan Wang et al. (2017) [80]	MRI	NR	NR	NO	Siamese neural network	CNN	NR	Clinical data collected from the Peking University Third Hospital	85,503/NR	NR	NO
Zhi-Long Wang et al. (2017) [81]	CT	YES	NR	YES	LS-SVM	SVM	NR	Clinical data collected from the Peking University Cancer Hospital & Institute, Beijing, China	66/65	2006.1–2012.1	NO
Tuan D. Pham et al. (2017) [82]*	CT	NR	NR	YES	Logistic regression; SVM; NBLDA	Logistic regression; SVM; NBLDA	NR	Retrospective cohort	NR/271	2010.4–2015.4	NO

Table 3 (*Continued*)

First author and year	Indicator definition				Algorithm			Data source			
	Method for predictor measurement	Exclusion of poor-quality imaging	Heatmap provided	Extracted features	Algorithm architecture name	Algorithm architecture	Transfer learning applied	Source of data	Number of images for training/testing	Data range	Open access data
Qi Zhang et al. (2017) [83]*	Real-time elastography and B-mode ultrasound	NR	NR	YES	SVM	SVM	NR	Retrospective cohort	NR/NR	2013.11–2014.11	NO
Yu-wen Wang et al. (2016) [84]*	MRI	NR	NR	YES	Feed-forward back-propagation NN	ANN	NR	Retrospective cohort	Stage I: 331/332 Stage II: 410/205	NR	NO
Ali Aslantas et al. (2016) [85]*	BS	NR	NR	YES	ANN	ANN	NR	Retrospective cohort from Medical Faculty of Suleyman Demirel University, Konya Education and Research Hospital	NR/130	2003–2013	NO
Aneta Chmielewski et al. (2015) [86]*	US	NR	NR	YES	SVM	SVM	NR	Retrospective cohort	80/25	NR	NO
Mitsuru Koizumi et al. (2015) [87]*	BS	NR	NR	YES	BONENAVI	ANN	NR	Retrospective cohort	NR/NR	2013.1–2013.12	NO
Mitsuru Koizumi et al. (2015) [88]	BS	NR	NR	YES	BONENAVI 2	ANN	NR	Retrospective cohort	NR/NR	2013.1–2013.12	NO
Nesrine Trabelsi et al. (2015) [89]	CT	NR	NR	YES	Neural network	Neural network	NR	Retrospective cohort	8/3	NR	NO
Xuan Gao et al. (2015) [90]	18F-FDG PET/CT	NR	NR	YES	RBF; SVM	SVM	NR	Retrospective cohort	30/30	2009.6–2013.7	NO
Osamu Tokuda et al. (2014) [91]*	BS	NR	NR	NO	BONENAVI	ANN	NR	NR	NR/3248	2006.1–2011.5	NO
Ari Seff et al. (2014) [92]	CT	NR	YES	YES	Random forest; SVM	Random forest; SVM	NR	NR	NR/984	NR	NO
Zhi-Guo Zhou et al. (2013) [93]*	MDCT	YES	NR	YES	ER based model	ER	NR	Retrospective cohort from Peking University Cancer Hospital & Institute (Beijing, China P. R.)	NR/NR	2006.4–2008.9	NO
Seungwook Yang et al. (2013) [94]*	Magnetic resonance black-blood imaging	NR	NR	YES	Conjugate gradient BP-ANN	ANN	NR	Retrospective cohort	37/53	NR	NO
Jianfei Liu et al. (2013) [95]	Abdominal contrast-enhanced CT	NR	NR	NO	Joint framework	NR	NR	Retrospective cohort	6/44	NR	NO
Yoshihiko Nakamura et al. (2013) [96]	3-D X-ray CT	NR	NR	YES	SVM	SVM	NR	Retrospective cohort	NR/NR	NR	NO
Chuan-Yu Chang et al. (2013) [97]	US	NR	NR	YES	PSONN; one-against-one multi-class SVM	SVM	NR	Retrospective cohort	88/89	2005–2007	NO
Johannes Feulner et al. (2013) [98]	CT	NR	NR	YES	Spatial prior; AdaBoost	Spatial prior; AdaBoost	NR	NR	289/1086	NR	NO
Chao Li et al. (2012) [99]	GSI-CT	NR	NR	YES	SFS-KNN; mRMR-KNN; Metric Learning	KNN	NR	Retrospective cohort from GE Healthcare equipment in Ruijin Hospital	NR/NR	2010.4	NO
Hongmin Cai et al. (2012) [100]	CT	NR	NR	YES	SVM	SVM	NR	Retrospective cohort	NR/228	2007.1–2008.11	NO
Shao-Jer Chen et al. (2012) [101]	US	NR	NR	YES	SVM	SVM	NR	Retrospective cohort from Buddhist Dalin Tzu Chi General Hospital	NR/NR	NR	NO

Table 3 (*Continued*)

First author and year	Indicator definition				Algorithm			Data source			
	Method for predictor measurement	Exclusion of poor-quality imaging	Heatmap provided	Extracted features	Algorithm architecture name	Algorithm architecture	Transfer learning applied	Source of data	Number of images for training/testing)	Data range	Open access data
Xiao-Peng Zhang et al. (2011) [102]*•	Multi-detector row CT	NR	NR	YES	LibSVM 2.89	SVM	NR	Retrospective cohort	NR/NR	2006.4–2008.9	NO
Matthias Dietzel et al. (2010) [103]	Breast MRI	NR	NR	YES	ANN	ANN	NR	Retrospective cohort	123/71	NR	NO
May Sadik et al. (2008) [104]•	BS	NR	NR	YES	ANN	ANN	NR	Retrospective cohort	810/59	Training: 1999.1–2002.6 Testing: 1999.8–2001.1	NO
Junji Shiraishi et al. (2008) [105]	Contrast-enhanced ultrasonography	NR	NR	YES	ANN	ANN	NR	Retrospective cohort	NR/NR	NR	NO
Junhua Zhang et al. (2008) [106]•	US	NR	NR	YES	v-SVM	SVM	NR	Retrospective cohort	NR/NR	2005.7–2006.6	NO
Rie Tagaya et al. (2008) [107]•	US from convex-type							echobronchoscopy	NR	NR	NO
BP-ANN	ANN	NR	Retro-spec-tive cohort from St.		Marianna University School of Medicine, Tokyo, Japan	9/82	2005.4–2007.3	NO			
K. Marten et al. (2004) [108]	MSCT	NR	NR	NR	NR	NR	NR	Retrospective cohort from Klinikum rechts der Isar, Technical University Munich, Germany	NR/NR	NR	NR

Abbreviation: NR=not reported. BS=bone scintigraphy. GC=gastric cancers. CT=computed tomography. MRI= magnetic resonance imaging. ANN= artificial neural network. SVM= support vector machine. NN= neural networks. CNN= convolutional neural networks. US= ultrasound. PSMA= Prostate specific-membrane antigen. 3D-T1-MPRAGE images=Three-dimensional T1 magnetization prepared rapid acquisition gradient echo. FR-CNN= fast region convolutional neural networks. CNN-*F*= CNN fast. PET: positron emission tomography. DNN= Deep neural network. MO= multi-objective model. KNN= *k* nearest neighbors. OCT= Optical coherence tomography. ANN= artificial neural network. BP-ANN= back-propagation artificial neural network. MSCT= multi-slice CT.

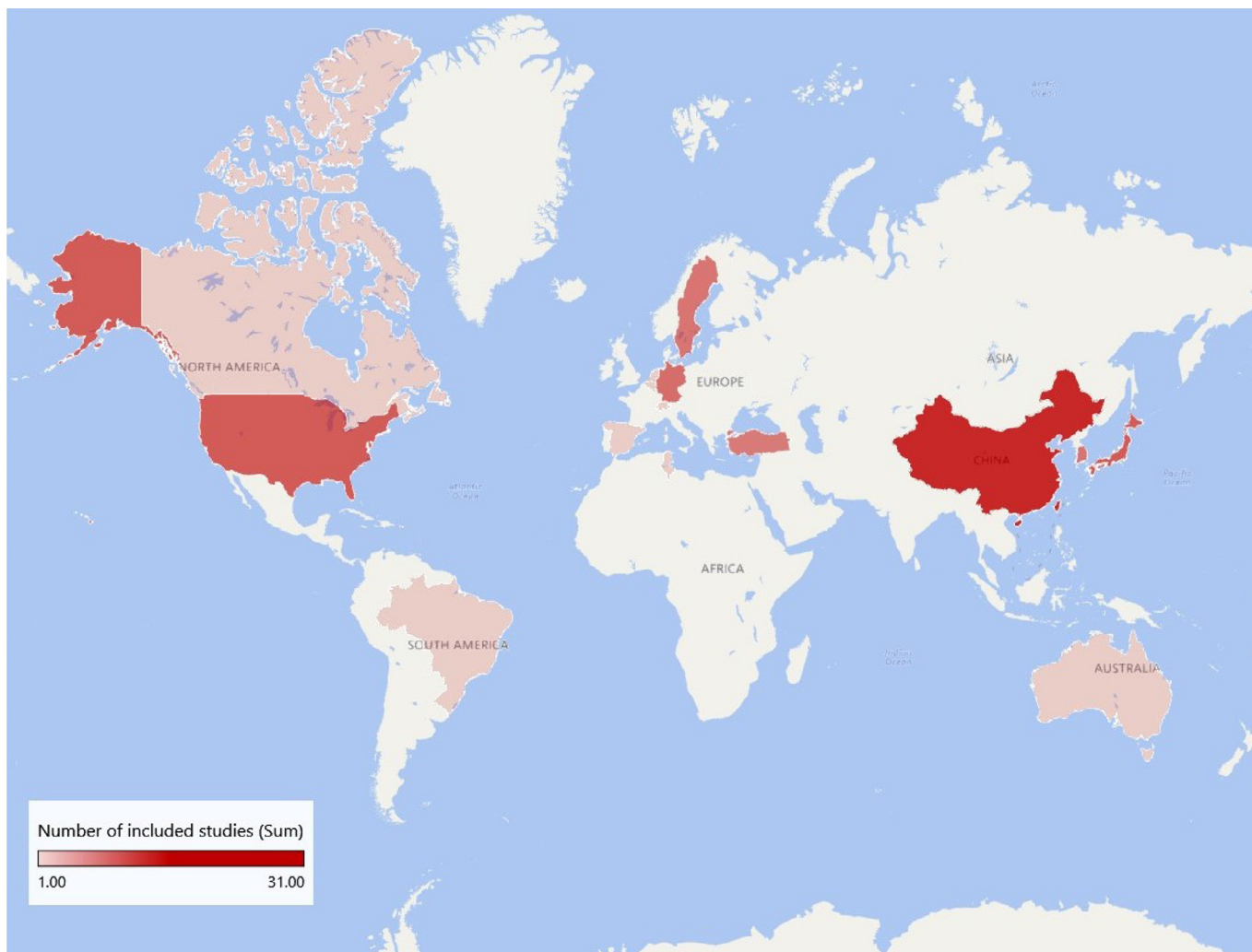• 34 studies included in the meta-analysis.

Fig. 2. International research situation.

ROC curves of these 34 studies (123 contingency tables) are shown in Fig. 3a, in which the pooled sensitivity was 82% (95% CI 79–84%) for all studies, and the pooled specificity was 84% (82–87%), with AUC of 0·90 (0·87–0·92). Many studies used more than one algorithm with several different accuracy for each algorithm. So, when selecting the contingency tables reporting the highest accuracy for different algorithms in these 34 studies with 48 tables, the pooled sensitivity was 87% (95% CI 84–89%), and the pooled specificity was 88% (84–92%), with AUC of 0·93(0·90–0·95) (Fig. 3b).

Considering different algorithms were used in the included studies, we divided them into ML algorithms (ANN, KNN, SVM, RF, logistic regression and decision tree) and DL algorithms (CNN, DNN and DCNN) and did separate analysis for them, which showed a pooled sensitivity of 87% (95% CI 83–90%) for ML and 86% (82–89%) for DL, and a pooled specificity of 89% (82–93%) for ML and 87% (82–91%) for DL (Fig. 4).

30 studies included in the meta-analysis were validated by in-sample dataset with a pooled sensitivity of 86% (95% CI 83–89%) and a pooled specificity of 90% (85–93%). Only 4 studies used out-of-sample dataset to perform an external validation, for which sensitivity was 89% (84–93%) and specificity was 74% (69–79%) (Fig. 5).

Of these 34 studies, 8 compared performance between AI algorithms and health-care professionals using the same sample, with 10 contingency tables for AI algorithm and 16 tables for health-care professionals (Fig. 6). The pooled sensitivity was 89% (95% CI 83–93%) for AI algorithms and 72% (61–81%) for health-care professionals.

The pooled specificity was 85% (79–89%) for AI algorithms and 72% (63–79%) for health-care professionals. Only 1 of the 8 studies was validated by out-of-sample dataset, and therefore a comparison between the performance of AI and health-care professionals by the identical external sample could not be performed.

All studies showed that the AI algorithms were beneficial for the diagnosis of tumor metastasis from medical radiology imaging when compared to the reference standard used in each study (OR 22·14 [95% CI 18·52–26·46] $P<0.001$, I^2=79·6%) (Fig. 7), from which we can also see high heterogeneity among these studies. Visual inspection of funnel plots suggested there was no publication bias ($P = 0.19$) (Supplementary figure 2).

To determine the source of heterogeneity, we did several subgroup analyses. In terms of metastasis types, there were DM whose pooled sensitivity was 88% (95% CI 80–93%), pooled specificity was 90% (76–96%), and AUC was 0·94 (0·92–0·97) ($n = 15$, I^2=79·7%, $P<0.001$) and LNM whose sensitivity was 86% (95% CI 83–88%), specificity was 87% (84–90%), and AUC was 0·93 (0·90–0·95) ($n = 33$, I^2=79·0%, $P<0.001$) (Fig. 8a). The outcomes were similar regarding the primary tumor types and medical imaging types. When it comes to the primary tumor types, in the breast cancer group, the sensitivity was 85% (95% CI 81–87%), the specificity was 82% (75–87%), and AUC was 0·86 (0·83–0·89) ($n = 12$, I^2=46.4·0%, $P = 0.039$). In the head and neck cancer group, the sensitivity was 87% (95% CI 81–91%), the specificity was 91% (87–94%), and AUC was 0·95 (0·92–0·96) ($n = 10$, I^2=77·8%, $P<0.001$). Regarding the
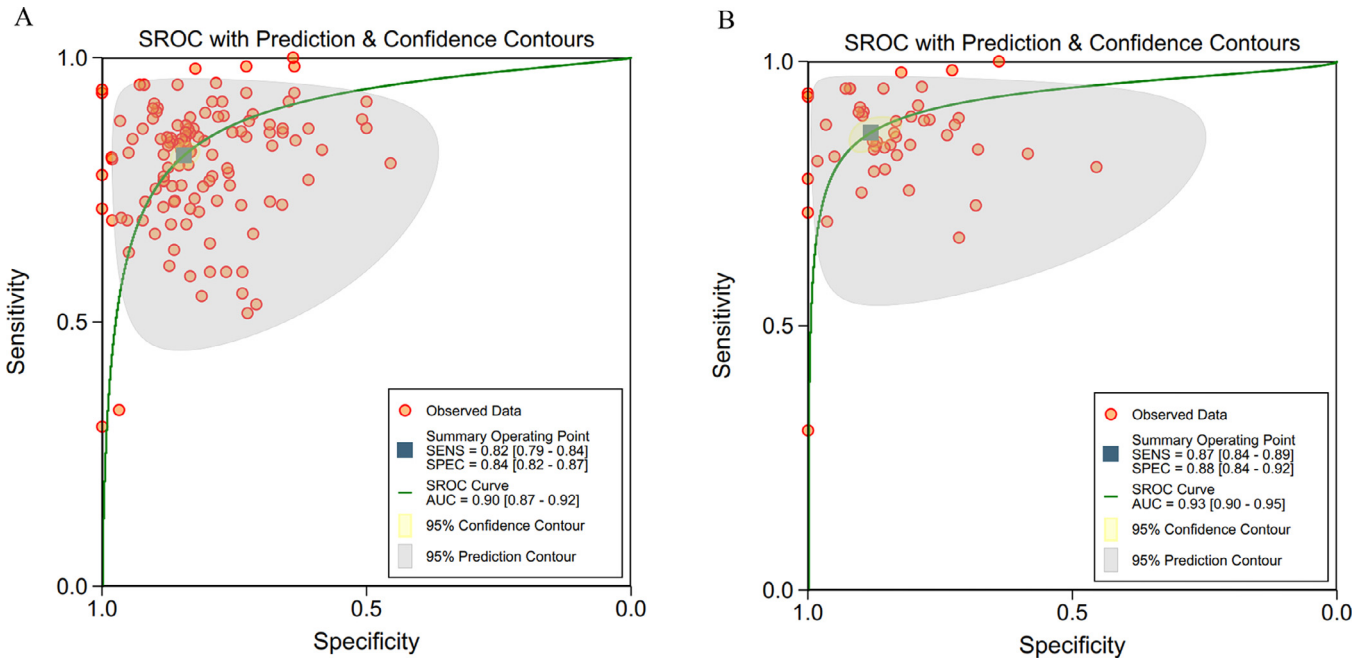
A

B

Fig. 3. (a, b). ROC curves of all studies included in the meta-analysis (34 studies)
   a: ROC curves of all studies included in the meta-analysis (34 studies with 123 tables)
   b: ROC curves of studies when selecting contingency tables reporting the highest accuracy (34 studies with 48 tables)
   Abbreviations: ROC=receiver operating characteristic; SENS= sensitivity; SPEC= specificity.

A

B
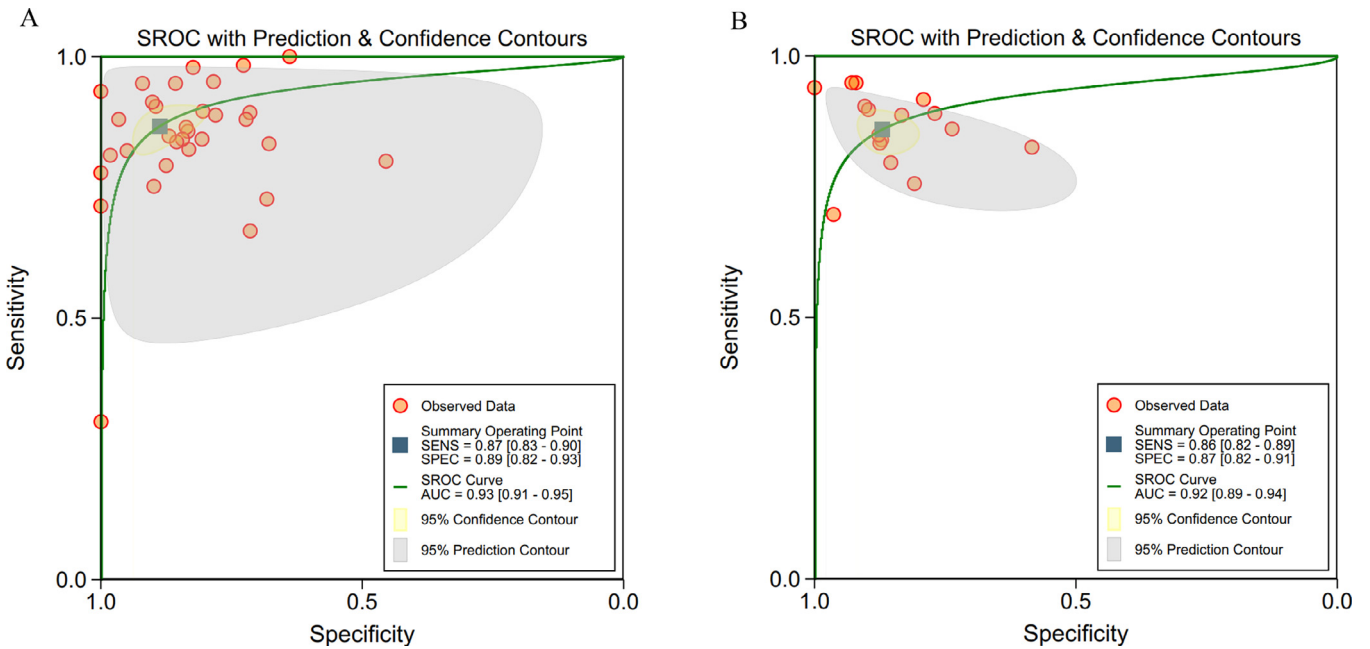
Fig. 4. (a, b): ROC curves of studies using different algorithms
   a: ROC curves of studies using machine learning algorithms (32 tables)
   b: ROC curves of studies using deep learning algorithms (16 tables).

other primary tumor types, the sensitivity was 88% (95% CI 83−91%), the specificity was 89% (81−94%), and AUC was 0·94 (0·91−0·95) ($n = 26$, I^2=84·2%, P<0·001) (Fig. 8b). As for medical imaging types, there were 16 contingency tables using CT (I^2=85·7%, P<0·001), 12 tables using ultra sound (I^2=0·0%, P = 0·505), 9 tables using bone scintigraphy (I^2=62·3%, P = 0·007), 6 tables using MRI (I^2=76·8%, P = 0·001) and 5 tables using other imaging types (I^2=65·6%, P = 0·02) (Fig. 8c). Subgroup analysis for

different AI algorithms contained ML ($n = 32$, I^2=82·4%, P<0·001) and DL ($n = 16$, I^2=70·8%, P<0·001). While in the studies were externally validated, heterogeneity was acceptable ($n = 7$, I^2=45·1%, P = 0·091). We could not find a reasonable explanation for heterogeneity from subgroup analysis. We also did regression analysis to find the sources of heterogeneity. However, the results also could not make an explanation (regression analysis results are provided in Supplementary table).
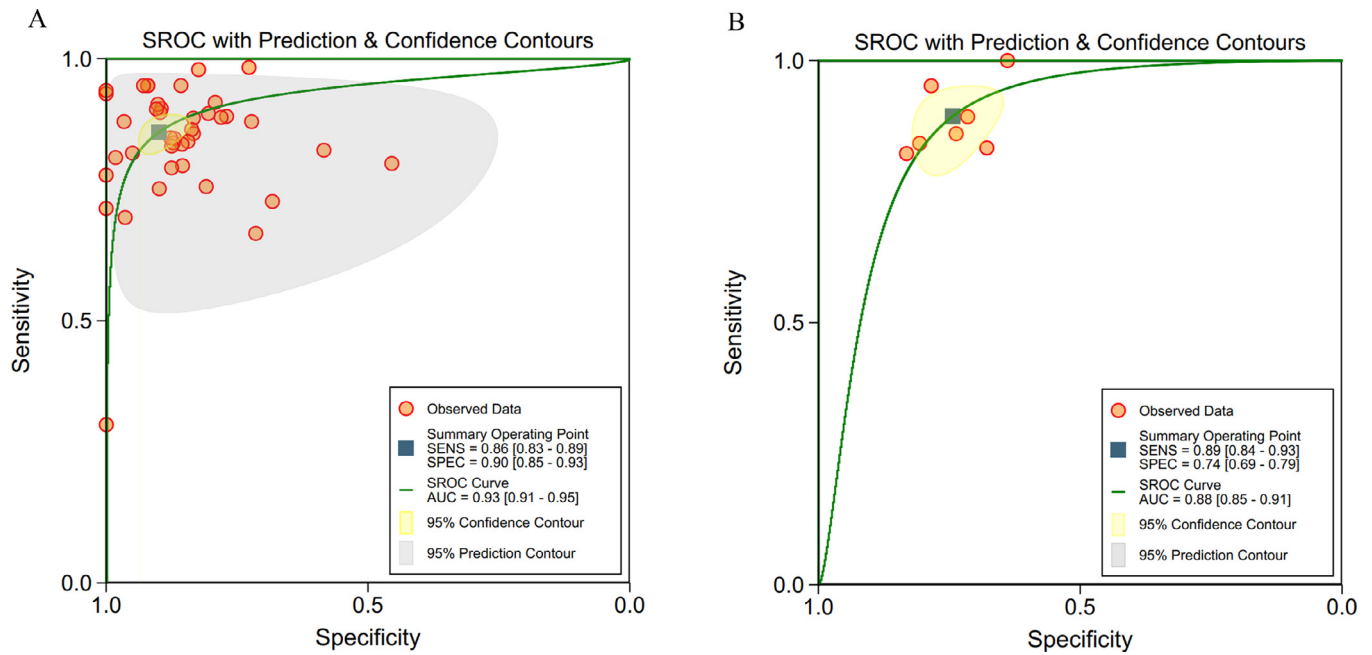
Fig. 5. (a, b): ROC curves of studies with or without external validation
  a: ROC curves of studies without external validation (41 tables)
  b: ROC curves of studies with external validation (7 tables).
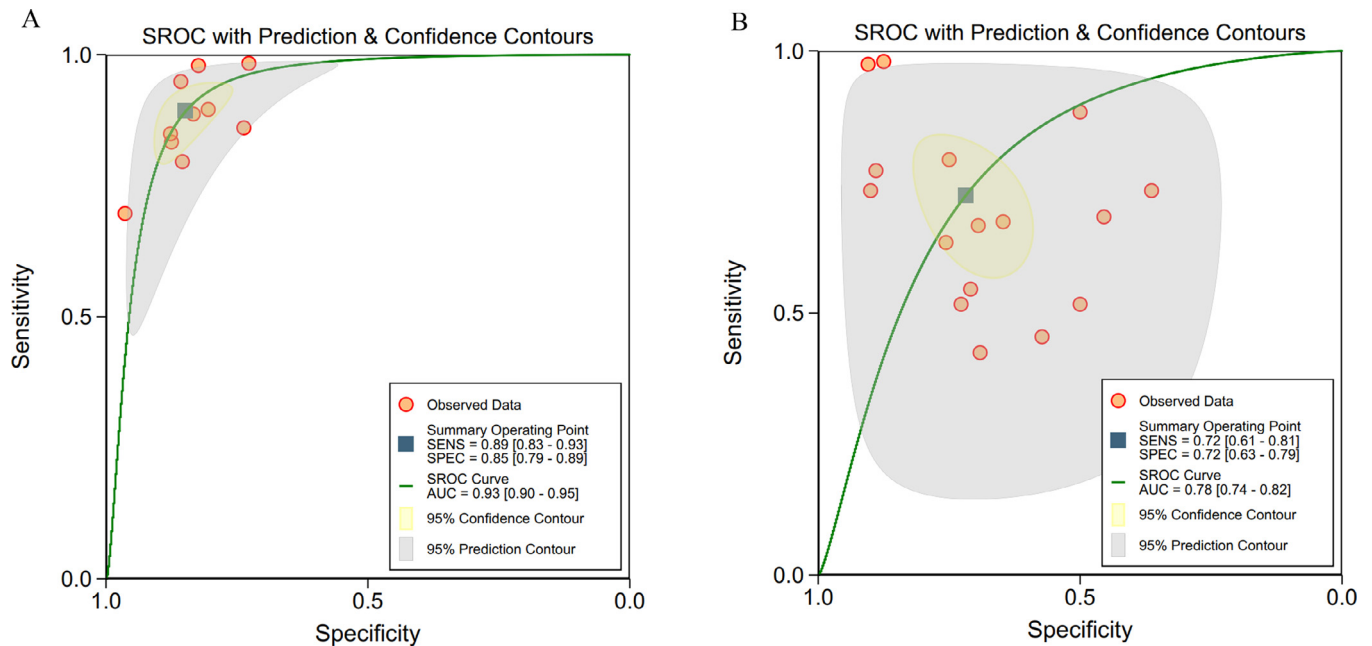
Fig. 6. (a, b). ROC curves of studies using the same sample for comparing performance between health-care professionals and artificial intelligence algorithms (8 studies)
  a: Artificial intelligence models (10 tables)
  b: Health-care professionals (16 tables).

4. Discussion

With great attention to the development of AI, more and more people are curious about its performance in medicine. In this systematic review and meta-analysis, we found that AI algorithms may be used for the diagnosis of tumor metastasis from medical radiology imaging material with equivalent or even better performance to health-care professionals, in terms of sensitivity and specificity. Tumor metastasis, as one of the main reasons for tumor-induced death, has a great impact on the treatment plan and prognosis judgment. Tumor metastasis sites may involve lymph nodes and distant organs, such as liver, lung and brain, which may be difficult to diagnose in clinical examination. Medical imaging is an important tool to diagnose tumor metastasis. However, the accurate diagnosis of tumor metastasis without misdiagnosis and missed diagnosis is a challenging task. The excellent performance of AI in image identification with rapid speed, high accuracy and significant manpower reduction excited the public. In 2019, Liu XX, et al. [30]. conducted a systematic review and meta-analysis and found the diagnostic performance of deep learning models from medical imaging to be equivalent to that of health-care professionals in classifying diseases, with the sensitivity of 87·0% and specificity of 92·5%, which provided the basis for the

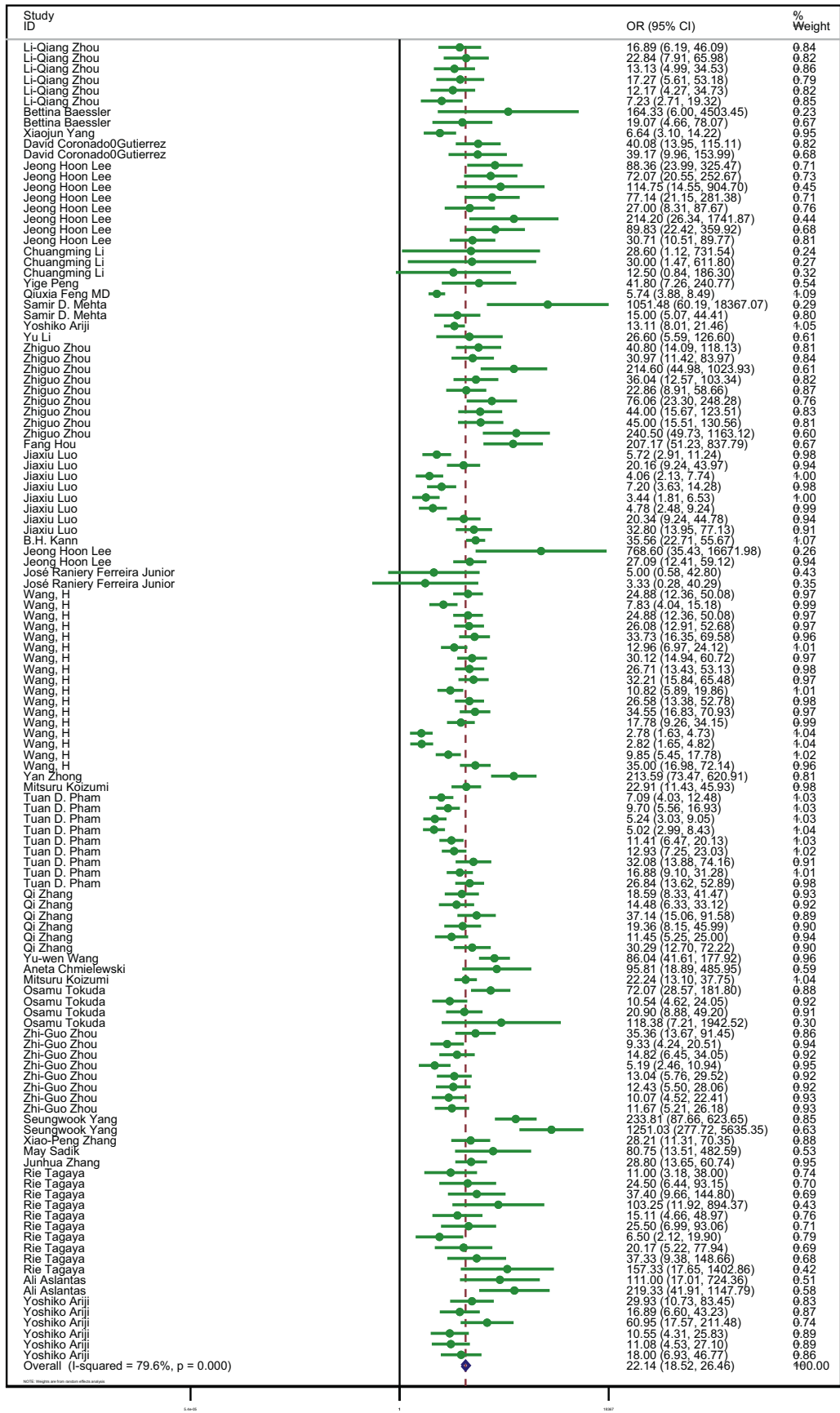| Study ID	OR (95% CI)	% Weight
Li-Qiang Zhou	16.89 (6.19, 46.09)	0.84
Li-Qiang Zhou	22.84 (7.91, 65.98)	0.82
Li-Qiang Zhou	13.13 (4.99, 34.53)	0.86
Li-Qiang Zhou	17.27 (5.61, 53.18)	0.79
Li-Qiang Zhou	12.17 (4.27, 34.73)	0.82
Li-Qiang Zhou	7.23 (2.71, 19.32)	0.85
Bettina Baessler	164.33 (6.00, 4503.45)	0.23
Bettina Baessler	19.07 (4.66, 78.07)	0.67
Xiaojun Yang	6.64 (3.10, 14.22)	0.95
David Coronado0Gutierrez	40.08 (13.95, 115.11)	0.82
David Coronado0Gutierrez	39.17 (9.96, 153.99)	0.68
Jeong Hoon Lee	88.36 (23.99, 325.47)	0.71
Jeong Hoon Lee	72.07 (20.55, 252.67)	0.73
Jeong Hoon Lee	114.75 (14.55, 904.70)	0.45
Jeong Hoon Lee	77.14 (21.15, 281.38)	0.71
Jeong Hoon Lee	27.00 (8.31, 87.67)	0.76
Jeong Hoon Lee	214.20 (26.34, 1741.87)	0.44
Jeong Hoon Lee	89.83 (22.42, 359.92)	0.68
Jeong Hoon Lee	30.71 (10.51, 89.77)	0.81
Chuangming Li	28.60 (1.12, 731.54)	0.24
Chuangming Li	30.00 (1.47, 611.80)	0.27
Chuangming Li	12.50 (0.84, 186.30)	0.32
Yige Peng	41.80 (7.26, 240.77)	0.54
Qiuxia Feng MD	5.74 (3.88, 8.49)	1.09
Samir D. Mehta	1051.48 (60.19, 18367.07)	0.29
Samir D. Mehta	15.00 (5.07, 44.41)	0.80
Yoshiko Ariji	13.11 (8.01, 21.46)	1.05
Yu Li	26.60 (5.59, 126.60)	0.61
Zhiguo Zhou	40.80 (14.09, 118.13)	0.81
Zhiguo Zhou	30.97 (11.42, 83.97)	0.84
Zhiguo Zhou	214.60 (44.98, 1023.93)	0.61
Zhiguo Zhou	36.04 (12.57, 103.34)	0.82
Zhiguo Zhou	22.86 (8.91, 58.66)	0.87
Zhiguo Zhou	76.06 (23.30, 248.28)	0.76
Zhiguo Zhou	44.00 (15.67, 123.51)	0.83
Zhiguo Zhou	45.00 (15.51, 130.56)	0.81
Zhiguo Zhou	240.50 (49.73, 1163.12)	0.60
Fang Hou	207.17 (51.23, 837.79)	0.67
Jiaxiu Luo	5.72 (2.91, 11.24)	0.98
Jiaxiu Luo	20.16 (9.24, 43.97)	0.94
Jiaxiu Luo	4.06 (2.13, 7.74)	1.00
Jiaxiu Luo	7.20 (3.63, 14.28)	0.98
Jiaxiu Luo	3.44 (1.81, 6.53)	1.00
Jiaxiu Luo	4.78 (2.48, 9.24)	0.99
Jiaxiu Luo	20.34 (9.24, 44.78)	0.94
Jiaxiu Luo	32.80 (13.95, 77.13)	0.91
B.H. Kann	35.56 (22.71, 55.67)	1.07
Jeong Hoon Lee	768.60 (35.43, 16671.98)	0.26
Jeong Hoon Lee	27.09 (12.41, 59.12)	0.94
José Raniery Ferreira Junior	5.00 (0.58, 42.80)	0.43
José Raniery Ferreira Junior	3.33 (0.28, 40.29)	0.35
Wang, H	24.88 (12.36, 50.08)	0.97
Wang, H	7.83 (4.04, 15.18)	0.99
Wang, H	24.88 (12.36, 50.08)	0.97
Wang, H	26.08 (12.91, 52.68)	0.97
Wang, H	33.73 (16.35, 69.58)	0.96
Wang, H	12.96 (6.97, 24.12)	1.01
Wang, H	30.12 (14.94, 60.72)	0.97
Wang, H	26.71 (13.43, 53.13)	0.98
Wang, H	32.21 (15.84, 65.48)	0.97
Wang, H	10.82 (5.89, 19.86)	1.01
Wang, H	26.58 (13.38, 52.78)	0.98
Wang, H	34.55 (16.83, 70.93)	0.97
Wang, H	17.78 (9.26, 34.15)	0.99
Wang, H	2.78 (1.63, 4.73)	1.04
Wang, H	2.82 (1.65, 4.82)	1.04
Wang, H	9.85 (5.45, 17.78)	1.02
Wang, H	35.00 (16.98, 72.14)	0.96
Yan Zhong	213.59 (73.47, 620.91)	0.81
Mitsuru Koizumi	22.91 (11.43, 45.93)	0.98
Tuan D. Pham	7.09 (4.03, 12.48)	1.03
Tuan D. Pham	9.70 (5.56, 16.93)	1.03
Tuan D. Pham	5.24 (3.03, 9.05)	1.03
Tuan D. Pham	5.02 (2.99, 8.43)	1.04
Tuan D. Pham	11.41 (6.47, 20.13)	1.03
Tuan D. Pham	12.93 (7.25, 23.03)	1.02
Tuan D. Pham	32.08 (13.88, 74.16)	0.91
Tuan D. Pham	16.88 (9.10, 31.28)	1.01
Tuan D. Pham	26.84 (13.62, 52.89)	0.98
Qi Zhang	18.59 (8.33, 41.47)	0.93
Qi Zhang	14.48 (6.33, 33.12)	0.92
Qi Zhang	37.14 (15.06, 91.58)	0.89
Qi Zhang	19.36 (8.15, 45.99)	0.90
Qi Zhang	11.45 (5.25, 25.00)	0.94
Qi Zhang	30.29 (12.70, 72.22)	0.90
Yu-wen Wang	86.04 (41.61, 177.92)	0.96
Aneta Chmielewski	95.81 (18.89, 485.95)	0.59
Mitsuru Koizumi	22.24 (13.10, 37.75)	1.04
Osamu Tokuda	72.07 (28.57, 181.80)	0.88
Osamu Tokuda	10.54 (4.62, 24.05)	0.92
Osamu Tokuda	20.90 (8.88, 49.20)	0.91
Osamu Tokuda	118.38 (7.21, 1942.52)	0.30
Zhi-Guo Zhou	35.36 (13.67, 91.45)	0.86
Zhi-Guo Zhou	9.33 (4.24, 20.51)	0.94
Zhi-Guo Zhou	14.82 (6.45, 34.05)	0.92
Zhi-Guo Zhou	5.19 (2.46, 10.94)	0.95
Zhi-Guo Zhou	13.04 (5.76, 29.52)	0.92
Zhi-Guo Zhou	12.43 (5.50, 28.06)	0.92
Zhi-Guo Zhou	10.07 (4.52, 22.41)	0.93
Zhi-Guo Zhou	11.67 (5.21, 26.18)	0.93
Seungwook Yang	233.81 (87.66, 623.65)	0.85
Seungwook Yang	1251.03 (277.72, 5635.35)	0.63
Xiao-Peng Zhang	28.21 (11.31, 70.35)	0.88
May Sadik	80.75 (13.51, 482.59)	0.53
Junhua Zhang	28.80 (13.65, 60.74)	0.95
Rie Tagaya	11.00 (3.18, 38.00)	0.74
Rie Tagaya	24.50 (6.44, 93.15)	0.70
Rie Tagaya	37.40 (9.66, 144.80)	0.69
Rie Tagaya	103.25 (11.92, 894.37)	0.43
Rie Tagaya	15.11 (4.66, 48.97)	0.76
Rie Tagaya	25.50 (6.99, 93.06)	0.71
Rie Tagaya	6.50 (2.12, 19.90)	0.79
Rie Tagaya	20.17 (5.22, 77.94)	0.69
Rie Tagaya	37.33 (9.38, 148.66)	0.68
Rie Tagaya	157.33 (17.65, 1402.86)	0.42
Ali Aslantas	111.00 (17.01, 724.36)	0.51
Ali Aslantas	219.33 (41.91, 1147.79)	0.58
Yoshiko Ariji	29.93 (10.73, 83.45)	0.83
Yoshiko Ariji	16.89 (6.60, 43.23)	0.87
Yoshiko Ariji	60.95 (17.57, 211.48)	0.74
Yoshiko Ariji	10.55 (4.31, 25.83)	0.89
Yoshiko Ariji	11.08 (4.53, 27.10)	0.89
Yoshiko Ariji	18.00 (6.93, 46.77)	0.86
Overall (I-squared = 79.6%, p = 0.000)	22.14 (18.52, 26.46)	100.00

NOTE: Weights are from random effects analysis

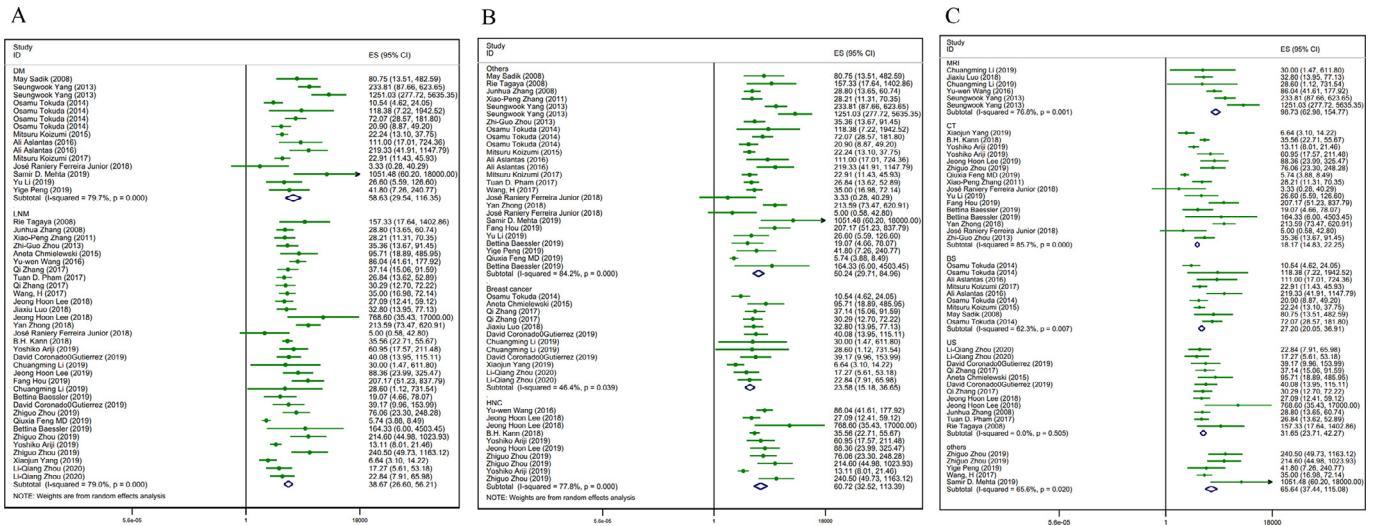**Fig. 7.** Forest plot of studies included in the meta-analysis (34 studies).

Fig. 8. (a, b, c). Forest plot of 3 subgroups
a: Subgroup 1. Different metastasis types
b: Subgroup 2. Different primary tumors
c: Subgroup 3. Different imaging types
Abbreviations: ES= estimate.

clinical use of deep learning models. As for the diagnosis of tumor metastasis, there were no other meta-analyses focus on this subject to date, where we also reached a similar positive conclusion.

The first appearance of AI as a term can be dated back to a conference in 1956 [31]. As a branch of computer science, AI attempted to use computers to simulate the thought processes and intelligent behaviors of people, of which machine learning is an important part. The presence of ANN, SVM and other ML algorithms aroused people's enthusiasm towards ML. It is not until 2006 that Geoffrey Hinton [13] the greatness of ML, proposed the concept of DL, which was the further development of ML. Twenty-three of the included studies in 2018 and beyond witnessed an increase in DL, in contrast to that only 1 study before 2018 involved in DL. Taking into account the different development stages of AI, we did a separate analysis for studies using different algorithms, where no significant difference was observed. This may be attributed to the small dataset of included studies, most of which collected a few hundred data, limiting the advantages of DL.

In our research, we observed statistically significant heterogeneity among the included studies. So, we did several subgroup analyses and meta-regression for different algorithms, existence of external validation, the type of metastasis, primary tumors and medical imaging. The heterogeneity of studies validated by external sample was acceptable. 3 of the 4 studies with external validation based on the different version of the same computer assisted diagnosis system, which may contribute to the result. Generally, the results still cannot explain the source of heterogeneity, which may be contributed to the broad nature of the review (accepting any classification task using any imaging types for any metastasis types of any primary tumors).

Although the outcome of our research seems to bring light to the application of AI in detecting tumor metastasis from medical radiology imaging, several common methodological defects should be noted.

First, the design and practice of some included studies may make the research results out of clinical practice, among which the most common is the lack of comparison with health-care professionals in diagnostic accuracy. In the 69 included studies, only 8 studies made a comparison with health-care professionals. Assessing the performance of AI in insolation instead of comparing with the most common way in clinical practice (review the medical imaging by a radiologist) makes the outcomes unreliable when applied in the clinical setting. Even if some studies had the comparison, very few of

them made it with humans using the same test dataset, resulting in a lack of comparability. Although we have reached the conclusion that AI models had the equivalent or even better diagnostic performance from medical imaging compared to health-care professionals, some factors still need to be considered. Only 8 studies using the same sample to compare health-care professionals and AI algorithms. Different studies recruited radiologists with different years of experience and different numbers. Some studies did not train radiologists in advance. All of above may influence the result. Furthermore, we included the studies that only used medical imaging to identify the presence of tumor metastasis, and excluded those that used other clinical materials, such as electronic medical record and clinical information of patients. It made our research topic more consistent. With the additional information available in the clinical practice, some prediction models can predict the possibility of metastasis based on the patient's gender, age and history to assist diagnosis [32−36].

Second, there were no prospective studies. All included studies were retrospective studies, whose participants were selected from hospital medical records. Some studies used online open-access datasets instead of being done in the real clinical environment. And some studies provided poor description of missing data. In terms of the standard to diagnose metastasis, some studies only used the opinion of a single radiologist as a standard, which may not be convincing.

Third, various indicators of diagnostic performance were used in the studies. The value of TP, TN, FP and FN at a specified threshold should at least be provided, but most studies did not give a threshold or explain the reason for choosing this threshold. Most studies set the threshold at the value of 0·5, which is a convention in machine learning development [37,38]. Indicators like the sensitivity, specificity and accuracy were used in most studies. When the number of patients with/without metastasis in the test dataset was reported, sensitivity and specificity can be used to calculate TP, TN, FP and FN for contingency tables construction. Other indicators such as precision, dice ratio, F1 score and recall, which are common in the field of computer science, also appeared as the only measure in some studies. However, these indicators are not comprehensive, only with which we cannot get enough information to construct contingency tables.

Last but not least, in the 69 included studies there were only 4 with external validation, which means testing the model with out-of-sample dataset from one or more other centers. Most studies split the dataset from one center into training set and test set randomly or

according to different time periods. The performance was evaluated by the test set, which should be called internal validation. Since the goal of validation is to investigate the performance within patients from different population, it is appropriate to collect a new dataset from different center. The absence of external validation made it hard to ensure the generalizability of the model, leading to overestimated results [39]. In our research, studies with external validation had an expectedly worse performance than internally validated studies. It is understandable that better performance can be achieved with the less heterogeneous samples. Strict external validation in the development of diagnostic model is urgently needed.

During the research, we also found some common deficiencies in AI studies. The most obvious point is that some key terminology is not uniformly named. Different studies have different definitions of the same terminology. For instance, for one AI model, the dataset is usually divided into several different parts, including the initial training set and one or more testing sets used to evaluate model effectiveness. While the term "validation" is used causally, some authors used this word to indicate the dataset used to test the diagnostic performance of the final model. Others defined it as a dataset with tuning function during the development process. The naming confusion makes it difficult to judge whether the test set is independent. The independent dataset, which is never learned by the model, is crucial to the credibility of the final model. So, canonical naming is urgently needed. Some scholars [30] have put forward suggestions. They distinguished the dataset used for a model as training set (for training the model), tuning set (for tuning the parameters of the model) and validation test set (for evaluating the performance of the final model), which is also accepted by our article. As for different types of validation test set, Altman and Royston's suggestion [39] may be adopted. They named dataset for in-sample validation as internal validation, dataset for in-sample validation with a temporal split as temporal validation, and dataset for out of sample validation as external validation. Studies on the AI application in the medical field should strive to avoid problems mentioned above in the future.

Diagnosis of tumor metastasis using AI algorithms has great potential. From this meta-analysis, we conservatively draw a conclusion that the AI algorithms may be used for the diagnosis of tumor metastasis from medical radiology imaging with equivalent or even better performance to health-care professionals, in terms of sensitivity and specificity, providing a basis for its clinical application. Its widespread clinical application may alleviate the shortage of medical resources, improve the detection rate and accuracy of tumor metastasis and then the prognosis of patients. However, it should be acknowledged that more high-quality studies on the AI application in the medical field with adaption to the clinical practice and standardized research routines are needed. In this review, we also put forward some existing problems of design and reporting that the algorithm developers should consider. High-quality studies are always the cornerstone of evaluation for diagnostic performance by various algorithms, which will finally benefit patients and the health care system.

Contributors

YL and GL contributed to the conception and design of the study. QZ, LY, JL and BZ contributed to the literature search and data extraction. QZ and KG contributed to risk of bias evaluation. BZ contributed to data analysis and interpretation. QZ wrote the first draft of the report with input from LY. All authors contributed to critical revision of the manuscript. All authors approved the manuscript.

Declaration of Competing Interest

All authors declare no competing interests.

Data sharing statement

The search strategy was shown in Appendix Section 1, and the contingency tables of 34 studies included in the meta-analysis were shown in Appendix Section 2. The results of risk of bias and publication bias were separately provided in the Supplementary Figure 1 and 2. Additional data are available on request.

Supplementary materials

Supplementary material associated with this article can be found in the online version at doi:10.1016/j.eclinm.2020.100669.

References

[1] Yamashita K, Hosoda K, Ema A, Watanabe M. Lymph node ratio as a novel and simple prognostic factor in advanced gastric cancer. Eur J Surg Oncol 2016;42(9):1253–60.
[2] O'Sullivan B, Brierley J, Byrd D, et al. The TNM classification of malignant tumours-towards common understanding and reasonable expectations. Lancet Oncol 2017;18(7):849–51.
[3] Ruytenberg T, Verbist BM, Vonk-Van Oosten J, Astreinidou E, Sjögren EV, Webb AG. Improvements in high resolution laryngeal magnetic resonance imaging for preoperative transoral laser microsurgery and radiotherapy considerations in early lesions. Front Oncol 2018;8:216.
[4] Tsili AC, Alexiou G, Naka C, Argyropoulou MI. Imaging of colorectal cancer liver metastases using contrast-enhanced US, multidetector CT, MRI, and FDG PET/CT: a meta-analysis. Acta Radiol 2020 284185120925481.
[5] Zhen L, Liu X, Yegang C, et al. Accuracy of multiparametric magnetic resonance imaging for diagnosing prostate Cancer: a systematic review and meta-analysis. BMC Cancer 2019;19(1):1244.
[6] Ozturk M, Selcuk MB, Polat AV, Ozbalci AB, Baris YS. The diagnostic value of ultrasound and shear wave elastography in the differentiation of benign and malignant soft tissue tumors. Skeletal Radiol 2020.
[7] Zhang L, Wang H, Li Q, Zhao M-H, Zhan Q-M. Big data and medical research in China. BMJ 2018;360:j5910.
[8] King BF. Artificial intelligence and radiology: what will the future hold? J Am Coll Radiol 2018;15(3 Pt B):501–3.
[9] Schlemmer H-P, Bittencourt LK, D'Anastasi M, et al. Global challenges for cancer imaging. J Glob Oncol 2018;4.
[10] Fukushima K. Neocognitron: a self organizing neural network model for a mechanism of pattern recognition unaffected by shift in position. Biol Cybern 1980;36(4):193–202.
[11] Cortes C, Vapnik V. Support-vector networks. Mach Learn 1995;20:273–97.
[12] The random subspace method for constructing decision forests -IEEE J Magazine [Internet]. [cited 2018 Jul 10]. Availablefrom: https://ieeexplore.ieee.org/document/709601/.
[13] Hinton GE, Osindero S, Teh Y-W. A fast learning algorithm for deep belief nets. Neural Comput 2006;18(7):1527–54.
[14] Hinton GE, Salakhutdinov RR. Reducing the dimensionality of data with neural networks. Science 2006;313(5786):504–7.
[15] Krizhevsky A, Sutskever I, Hinton GJ. Ainips. ImageNet classification with deep convolutional. Neural Netw 2012;25(2).
[16] Litjens G, Kooi T, Bejnordi BE, et al. A survey on deep learning in medical image analysis. Med Image Anal 2017;42:60–88.
[17] Rajkomar A, Lingam S, Taylor AG, Blum M, Mongan J. High-throughput classification of radiographs using deep convolutional neural networks. J Digit Imaging 2017;30(1).
[18] Vamathevan J, Clark D, Czodrowski P, et al. Applications of machine learning in drug discovery and development. Nat Rev Drug Discov 2019;18(6):463–77.
[19] Vinyals O, Toshev A, Bengio S, Erhan D. Show and tell: lessons learned from the 2015 MSCOCO image captioning challenge. IEEE Trans Pattern Anal Mach Intell 2017;39(4):652–63.
[20] Cao C, Liu F, Tan H, et al. Deep learning and its applications in biomedicine. Geno Proteomics Bioinform 2018;16(1):17–32.
[21] Anthimopoulos M, Christodoulidis S, Ebner L, Christe A, Mougiakakou S. Lung pattern classification for interstitial lung diseases using a deep convolutional neural network. IEEE Trans Med Imaging 2016;35(5):1207–16.
[22] Xu Y, Hosny A, Zeleznik R, et al. Deep learning predicts lung cancer treatment response from serial medical imaging. Clin Cancer Res 2019;25(11):3266–75.
[23] Kooi T, Litjens G, van Ginneken B, et al. Large scale deep learning for computer aided detection of mammographic lesions. Med Image Anal 2017;35:303–12.
[24] Yang X, Kwitt R, Styner M, Niethammer M. Quicksilver: fast predictive image registration - a deep learning approach. Neuroimage 2017;158:378–96.

[25] Hosny A, Parmar C, Quackenbush J, Schwartz LH, Aerts HJWL. Artificial intelligence in radiology. Nat Rev Cancer 2018;18(8):500–10.

[26] Ensmenger N. Is chess the drosophila of artificial intelligence? A social history of an algorithm. Soc Stud Sci 2012;42(1):5–30.

[27] Moher D, Liberati A, Tetzlaff J, Altman DG, PRISMA Group. Preferred reporting items for systematic reviews and meta-analyses: the PRISMA statement. BMJ 2009;339:b2535.

[28] Moons KG, de Groot JA, Bouwmeester W, et al. Critical appraisal and data extraction for systematic reviews of prediction modelling studies: the CHARMS checklist. PLoS Med 2014;11(10):e1001744.

[29] Whiting PF, Rutjes AW, Westwood ME, Mallett S, Deeks JJ, Reitsma JB, Leeflang MM, Sterne JA, Bossuyt PM, QUADAS-2 Group. QUADAS-2: a revised tool for the quality assessment of diagnostic accuracy studies. Ann Intern Med 2011;155 (8):529–36.

[30] Liu XX, Faes L, Kale AU, et al. A comparison of deep learning performance against health-care professionals in detecting diseases from medical imaging: a systematic review and meta-analysis. Lancet Digit Health 2019;1(6):E271–E97.

[31] Miller RA. Medical diagnostic decision support systems–past, present, and future: a threaded bibliography and brief commentary. J Am Med Inform Ass 1994;1:8–27.

[32] Liu T, Ge X, Yu J, et al. Comparison of the application of B-mode and strain elastography ultrasound in the estimation of lymph node metastasis of papillary thyroid carcinoma based on a radiomics approach. Int J Comput Assist Radiol Surg 2018;13(10):1617–27.

[33] Ozden S, Er S, Saylam B, Yildiz BD, Senol K, Tez M. A comparison of logistic regression and artificial neural networks in predicting central lymph node metastases in papillary thyroid microcarcinoma. Ann Ital Chir 2018;89:193–8.

[34] Nowikiewicz T, Wnuk P, Małkowski B, Kurylcio A, Kowalewski J, Zegarski W. Application of artificial neural networks for predicting presence of non-sentinel lymph node metastases in breast cancer patients with positive sentinel lymph node biopsies. Arch Med Sci 2017;13(6):1399–407.

[35] Qiu C, Jiang L, Cao Y, Hu C, Yu Y, Zhang HJTCR. Factors associated with de novo metastatic disease in invasive breast cancer: comparison of artificial neural network and logistic regression models. 2019 2019;8(1):77–86.

[36] Vaquero-Garcia J, Lalonde E, Ewens KG, et al. PRiMeUM: a model for predicting risk of metastasis in uveal melanoma. Invest Ophthalmol Vis Sci 2017;58 (10):4096–105.

[37] Lin H, Chen H, Graham S, Dou Q, Rajpoot N, Heng PA. Fast ScanNet: fast and dense analysis of multi-gigapixel whole-slide images for cancer metastasis detection. IEEE Trans Med Imaging 2019;38(8):1948–58.

[38] Bhooshan N, Giger ML, Jansen SA, Li H, Lan L, Newstead GM. Cancerous breast lesions on dynamic contrast-enhanced MR images: computerized characterization for image-based prognostic markers. Radiology 2010;254(3):680–90.

[39] Altman DG, Royston P. What do we mean by validating a prognostic model. Stat Med 2000;19(4):453–73.

[40] Koizumi M, Motegi K, Koyama M, et al. Diagnostic performance of a computer-assisted diagnostic system: sensitivity of BONENAVI for bone scintigraphy in patients with disseminated skeletal metastasis is not so high. Ann Nucl Med 2020.

[41] Li J, Dong D, Fang M, et al. Dual-energy CT-based deep learning radiomics can improve lymph node metastasis risk prediction for gastric cancer. Eur Radiol 2020.

[42] Zhang L, Ren Z. Comparison of CT and MRI images for the prediction of soft-tissue sarcoma grading and lung metastasis via a convolutional neural networks model. Clin Radiol 2020;75(1):64–9.

[43] Zhou L Q, Wu XL, Huang SY, et al. Lymph node metastasis prediction from primary breast cancer US images using deep learning. Radiology 2020;294(1):19–28.

[44] Grovik E, Yi D, Iv M, Tong E, Rubin D, Zaharchuk G. Deep learning enables automatic detection and segmentation of brain metastases on multisequence MRI. J Magnetic Resonance Img 2020;51(1):175–82.

[45] Zhao Y, Gafita A, Tetteh G, et al. Deep neural network for automatic characterization of lesions on 68Ga-PSMA PET/CT Images. Conference proceedings: annual international conference of the IEEE engineering in medicine and biology society IEEE engineering in medicine and biology society annual conference, 2019; 2019. p. 951–4.

[46] Xue J, Wang B, Ming Y, et al. Deep-learning-based detection and segmentation-assisted management on brain metastases. Neuro-oncology 2019.

[47] Baessler B, Nestler T, Pinto Dos Santos D, et al. Radiomics allows for detection of benign and malignant histopathology in patients with metastatic testicular germ cell tumors prior to post-chemotherapy retroperitoneal lymph node dissection. Eur Radiol 2019.

[48] Yang X, Wu L, Ye W, et al. Deep learning signature based on staging ct for preoperative prediction of sentinel lymph node metastasis in breast cancer. Acad Radiol 2019.

[49] Gao Y, Zhang Z-D, Li S, et al. Deep neural network-assisted computed tomography diagnosis of metastatic lymph nodes from gastric cancer. Chin Med J 2019;132(23):2804–11.

[50] Coronado-Gutierrez D, Santamaria G, Ganau S, et al. Quantitative ultrasound image analysis of axillary lymph nodes to diagnose metastatic involvement in breast cancer. Ultrasound Med Biol 2019;45(11):2932–41.

[51] Okada Y, Matsushita S, Nakajima Y, et al. Comparison of diagnostic precision for bone metastasis of primary breast cancer between BONENAVI version 1 and BONENAVI version 2. Nucl Med Commun 2019;40(11):1148–53.

[52] Lee JH, Ha EJ, Kim JH. Application of deep learning to the diagnosis of cervical lymph node metastasis from thyroid cancer with CT. Eur Radiol 2019;29 (10):5452–7.

[53] Jansen MJA, Kuijf HJ, Niekel M, et al. Liver segmentation and metastases detection in MR images using convolutional neural networks. J Med Img (Bellingham, Wash) 2019;6(4):044003 -.

[54] Liu J, Sun D, Chen L, et al. Radiomics analysis of dynamic contrast-enhanced magnetic resonance imaging for the prediction of sentinel lymph node metastasis in breast cancer. Front Oncol 2019;9(980).

[55] Dohopolski M, Chen L, Sher DJ, Wang J. Predicting lymph node metastasis in patients with oropharyngeal cancer by convolutional neural networks with associated epistemic uncertainty. Int J Radiation Oncol Biol Phys 2019;105S(1): S122. -S.

[56] Peng Y, Bi L, Guo Y, Feng D, Fulham M, Kim J. Deep multi-modality collaborative learning for distant metastases predication in PET-CT soft-tissue sarcoma studies. Conference proceedings: annual international conference of the IEEE engineering in medicine and biology society IEEE engineering in medicine and biology society annual conference, 2019; 2019. p. 3658–88.

[57] Feng Q-X, Liu C, Qi L, et al. An intelligent clinical decision support system for preoperative prediction of lymph node metastasis in gastric cancer. J Am College Radiol 2019;16(7):952–60.

[58] Schnelldorfer T, Ware MP, Liu LP, Sarr MG, Birkett DH, Ruthazer R. Can we accurately identify peritoneal metastases based on their appearance? an assessment of the current practice of intraoperative gastrointestinal cancer staging. Ann Surg Oncol 2019;26(6):1795–804.

[59] Mehta SD, Sebro R. Random forest classifiers aid in the detection of incidental osteoblastic osseous metastases in DEXA studies. Int J Comput Assist Radiol Surg 2019;14(5):903–9.

[60] Ariji Y, Fukuda M, Kise Y, et al. Contrast-enhanced computed tomography image assessment of cervical lymph node metastasis in patients with oral cancer by using a deep learning system of artificial intelligence. Oral Surg Oral Med Oral Pathol Oral Radiol 2019;127(5):458–63.

[61] Zhou YP, Li S, Zhang XX, et al. High definition MRI rectal lymph node aided diagnostic system based on deep neural network. Zhonghua Wai Ke Za Zhi 2019;57 (2):108–13.

[62] Li Y, Eresen A, Shangguan J, et al. Establishment of a new non-invasive imaging prediction model for liver metastasis in colon cancer. Am J Cancer Res 2019;9 (11):2482–92.

[63] Zhiguo Z, Dohopolski M, Liyuan C, et al. Reliable lymph node metastasis prediction in head & neck cancer through automated multi-objective model. 2019: 4.

[64] Acar E, Leblebici A, Ellidokuz BE, Basbinar Y, Kaya GC. Machine learning for differentiating metastatic and completely responded sclerotic bone lesion in prostate cancer: a retrospective radiomics study. Br J Radiol 2019;92 (201902861101).

[65] Hou F, Yang Z, Gu W, Yu Y, Liang Y. OCT Automatic identification of metastatic lymph nodes in OCT images. In: Fujimoto JG, Izatt JA, editors. Proceedings of SPIE; 2019.

[66] Ariji YA-OH, Sugita Y, Nagao T, et al. CT evaluation of extranodal extension of cervical lymph node metastases in patients with oral squamous cell carcinoma using deep learning classification. doi:10.1007/s11282-019-00391-4.

[67] Xu X, Li H, Wang S, et al. Multiplanar MRI-Based predictive model for preoperative assessment of lymph node metastasis in endometrial cancer.

[68] Luo J, Ning Z, Zhang S, Feng Q, Zhang Y. Bag of deep features for preoperative prediction of sentinel lymph node metastasis in breast cancer. Phys Med Biol 2018;63(24501424).

[69] Ha R, Chang P, Karcich J, et al. Axillary lymph node evaluation utilizing convolutional neural networks using MRI dataset. J Digit Imaging 2018;31(6):851–6.

[70] Kann BH, Aneja S, Loganadane GV, et al. Successful identification of head and neck cancer (HNC) nodal metastasis (NM) and extranodal extension (ENE) using deep learning neural networks. Int J Radiation Oncol Biol Phys 2018;102S(3): S60. -S.

[71] Lee JH, Baek JH, Kim JH, et al. Deep learning-based computer-aided diagnosis system for localization and diagnosis of metastatic lymph nodes on ultrasound: a pilot study. THYROID 2018;28(10):1332–8.

[72] Lu Y, Yu Q, Gao Y, et al. Identification of metastatic lymph nodes in MR imaging with faster region-based convolutional neural networks. Cancer Res. 2018;78 (17):5135–43.

[73] Ferreira Junior JR, Koenigkam-Santos M, Garcia Cipriano FE, Fabro AT, de Azevedo-Marques PM. Radiomics-based features for pattern recognition of lung cancer histopathology and metastases. Comput Methods Programs Biomed 2018;159:23–30.

[74] Lo T-Y, Wei P-Y, Yen C-H, et al. Prediction of metastasis in head and neck cancer from computed tomography images. 2018: 18–23.

[75] Jin L, Peng W, Yanzhao L, Yang Z, Xiaolong L, Kuan L. Transfer learning of pretrained inception-v3 model for colorectal cancer lymph node metastasis classification. 2018: 1650–4.

[76] Larhmam MA, Mahmoudi S, Drisis S, Benjelloun M. A Texture analysis approach for spine metastasis classification in T1 and T2 MRI. In: Rojas I, Ortuno F, editors; 2018: 198–211.

[77] Zhong Y, Yuan M, Zhang T, Zhang YD, Li H, Yu TF. Radiomics approach to prediction of occult mediastinal lymph node metastasis of lung adenocarcinoma.

[78] Wang H, Zhou Z, Li Y, et al. Comparison of machine learning methods for classifying mediastinal lymph node metastasis of non-small cell lung cancer from 18F-FDG PET/CT images. EJNMMI Res 2017;7(1):11.

[79] Koizumi M, Motegi K, Koyama M, Terauchi T, Yuasa T, Yonese J. Diagnostic performance of a computer-assisted diagnosis system for bone scintigraphy of

newly developed skeletal metastasis in prostate cancer patients: search for low-sensitivity subgroups. Ann Nucl Med 2017;31(7):521–8.

[80] Wang J, Fang Z, Lang N, Yuan H, Su M-Y, Baldi P. A multi-resolution approach for spinal metastasis detection using deep Siamese neural networks. Comput. Biol. Med. 2017;84:137–46.

[81] Wang Z-L, Zhou Z-G, Chen Y, Li X-T, Sun Y-S. Support vector machines model of computed tomography for assessing lymph node metastasis in esophageal cancer with neoadjuvant chemotherapy. J Comput Assist Tomogr 2017;41(3):455–60.

[82] Pham TD, Watanabe Y, Higuchi M, Suzuki H. Texture analysis and synthesis of malignant and benign mediastinal lymph nodes in patients with lung cancer on computed tomography. Sci Rep 2017;7(43209).

[83] Zhang Q, Suo J, Chang W, Shi J, Chen M. Dual-modal computer-assisted evaluation of axillary lymph node metastasis in breast cancer patients on both real-time elastography and B-mode ultrasound.

[84] Wang Y-W, Wu C-S, Zhang G-Y, et al. Can parameters other than minimal axial diameter in mri and pet/ct further improve diagnostic accuracy for equivocal retropharyngeal lymph nodes in nasopharyngeal carcinoma. PLoS ONE 2016;11 (e016374110).

[85] Aslantas A, Dandil E, Saglam S, Cakiroglu M. CADBOSS: a computer-aided diagnosis system for whole-body bone scintigraphy scans.

[86] Chmielewski A, Dufort P, Scaranelo AM. A computerized system to assess axillary lymph node malignancy from sonographic images. Ultrasound Med Biol 2015;41(10):2690–9.

[87] Koizumi M, Miyaji N, Murata T, et al. Evaluation of a revised version of computer-assisted diagnosis system, BONENAVI version 2.1.7, for bone scintigraphy in cancer patients. Ann Nucl Med 2015;29(8):659–65.

[88] Koizumi M, Wagatsuma K, Miyaji N, et al. Evaluation of a computer-assisted diagnosis system, BONENAVI version 2, for bone scintigraphy in cancer patients in a routine clinical setting. Ann Nucl Med 2015;29(2):138–48.

[89] Trabelsi N, Ben Sellem D. Comparison of supervised and unsupervised classifications in the detection of hepatic metastases. 2015.

[90] Gao X, Chu C, Li Y, et al. The method and efficacy of support vector machine classifiers based on texture features and multi-resolution histogram from (18)F-FDG PET-CT images for the evaluation of mediastinal lymph nodes in patients with lung cancer.

[91] Tokuda O, Harada Y, Ohishi Y, Matsunaga N, Edenbrandt L. Investigation of computer-aided diagnosis system for bone scans: a retrospective analysis in 406 patients. Ann Nucl Med 2014;28(4):329–39.

[92] Seff A, Lu L, Cherry KM, et al. 2D view aggregation for lymph node detection using a shallow hierarchy of linear classifiers. In: Golland P, Hata N, Barillot C, Hornegger J, Howe R, editors. Lecture notes in computer science; 2014. p. 544–52.

[93] Zhou Z-G, Liu F, Jiao L C, et al. An evidential reasoning based model for diagnosis of lymph node metastasis in gastric cancer. BMC Med Inform Decis Mak 2013;13 (123).

[94] Yang S, Nam Y, Kim M-O, Kim EY, Park J, Kim D H. Computer-aided detection of metastatic brain tumors using magnetic resonance black-blood imaging. Invest Radiol 2013;48(2):113–9.

[95] Liu J, Wang S, Linguraru MG, Yao J, Summers RM. A Variational framework for joint detection and segmentation of ovarian cancer metastases. In: Sakuma I, Barillot C, Navab N, editors. Lecture notes in computer science; 2013. p. 83–90.

[96] Nakamura Y, Nimura Y, Kitasaka T, et al. Automatic abdominal lymph node detection method based on local intensity structure analysis from 3D X-ray CT images. In: Novak CL, Aylward S, editors. Proceedings of SPIE; 2013.

[97] Chang C-Y, Lai C-C, Lai C-T, Chen S-J. Integrating PSONN and Boltzmann function for feature selection and classification of lymph nodes in ultrasound images. J Vis Commun Image Represent 2013;24(1):23–30.

[98] Feulner J, Zhou Sk Fau Hammon M, Hammon M, Fau Hornegger J, Hornegger J, Fau Comaniciu D, Comaniciu D. Lymph node detection and segmentation in chest CT data using discriminative learning and a spatial prior.

[99] Li C, Zhang S, Zhang H, et al. Using the K-nearest neighbor algorithm for the classification of lymph node metastasis in gastric cancer. Comput Math Methods Med 2012(876545).

[100] Cai H, Cui C Fau Tian H, Tian H Fau Zhang M, Zhang M Fau Li L, Li L. A novel approach to segment and classify regional lymph nodes on computed tomography images.

[101] Chen SJ, Lin Ch Fau Chang C-Y, Chang Cy Fau Chang K-Y, et al. Characterizing the major sonographic textural difference between metastatic and common benign lymph nodes using support vector machine with histopathologic correlation.

[102] Zhang X-P, Wang Z-L, Tang L, Sun Y-S, Cao K, Gao Y. Support vector machine model for diagnosis of lymph node metastasis in gastric cancer with multidetector computed tomography: a preliminary study. BMC Cancer 2011;11(10).

[103] Dietzel M, Baltzer PAT, Dietzel A, et al. Application of artificial neural networks for the prediction of lymph node metastases to the ipsilateral axilla - initial experience in 194 patients using magnetic resonance mammography. Acta radiol 2010;51(8):851–8.

[104] Sadik M, Hamadeh I, Nordblom P, et al. Computer-assisted interpretation of planar whole-body bone scans. J Nuclear Med 2008;49(12):1958–65.

[105] Shiraishi J, Sugimoto K, Moriyasu F, Kamiyama N, Doi K. Computer-aided diagnosis for the classification of focal liver lesions by use of contrast-enhanced ultrasonography. Med Phys 2008;35(5):1734–46.

[106] Zhang J, Wang Y, Dong Y, Wang Y. Computer-aided diagnosis of cervical lymph nodes on ultrasonography. Comput. Biol. Med. 2008;38(2):234–43.

[107] Tagaya R, Kurimoto N, Osada H, Kobayashi A. Automatic objective diagnosis of lymph nodal disease by B-mode images from convex-type echobronchoscopy. Chest 2008;133(1):137–42.

[108] Marten K, Grillhosl A, Fau Seyfarth T, Seyfarth T, Fau Obenauer S, Obenauer S, Fau Rummeny EJ, Rummeny Ej Fau Engelke C, Engelke C. Computer-assisted detection of pulmonary nodules: evaluation of diagnostic performance using an expert knowledge-based detection system with variable reconstruction slice thickness settings.